UNIVERSITY OF PAVIA

Psychology, Neuroscience and Data Science Programme

Radiology Department

Ph.D. THESIS IN RADIOLOGICAL AND IMAGING SCIENCES

XXXIII CYCLE

Non-Contrast MR-Lymphography: New Tool for Evaluating Lymphedema Pre and Post-Lymph nodal Autotransplantation

Supervisor: Prof. Fabrizio Calliada

Author: Abdullah ALMUJALLY

Dedication

To my beloved family

Acknowledgment

First of all, I would like to thank my supervisor Professor Fabrizio Calliada, for supervising this work, for the invaluable comments, professional recommendations and providing me with the outstanding technical guidance throughout this thesis. I appreciate his support, patience, and encouraging me all times to accomplish my work nicely. He is always available to me unconditionally to support, guide and motivate me throughout my studies as well as touring me to the valuable sources.

I also extend my great appreciation to the Lymph Team: IRCCS Policlinico San Matteo (PV) at radiology department, University of Pavia. I am thankful to the staff at the MRI unit who helped me in data collection with a pleasure and extended an unfailing cooperation. Their technical accuracy is at another level.

I would like to express my sincere gratitude to King Faisal Specialist Hospital & Research Centre, Riyadh, Saudi Arabia for the scholarship to peruse my PhD study in this wonderful university.

Finally, I am also thankful to my family and friends for their support and encouragement.

Contents

No.	Item	Page No.
	Dedication	II
	Acknowledgements	III
	Contents	IV
	Abstract	V
	Chapters	
1	Introduction	1
2	Theoretical Background	19
3	Materials and Methods	50
4	Results and Discussion	62
5	Conclusions	81
	Biography	82

Abstract:

MR lymphangiography using dynamic contrast-enhanced images is useful in providing high quality images to diagnose many clinical conditions. However, this procedure cannot be used for traumatic patients or patients with severe side effect of using contrast media. Thus, the only option available is to develop a protocol for lymphedema without contrast agents in order to reduce the contra indication of the procedure and to extract diagnostic information without contrast medium. The objectives of this study are to evaluate the role of MR-lymphographic for the assessment of lymphedema before and after lymph node self-transplantation. This study was conducted at IRCCS Policlinico San Matteo (PV), Pavia, Italy. A total of 17 patients were investigated for lymphedema evaluation due to primary or secondary lymphedema. All procedures were performed due to justified clinical conditions according to the ethical guidelines. All procedures were performed using two MRI machines: Siemens Magnetom Aera 1.5T and Philips Ingenia 1.5 T. Early Lymphedema stages diagnosis represents great challenges. Non contrast MRL is used to diagnose accurately the lymphatic system disorder. From studies, the researchers have found non contrast MRL is as a promising methodology in the diagnosis of lymphatic system disorders with accuracy up to 90%. This research findings reveal that non-contrast MRL imaging technique can increase the accuracy of lymphedema diagnosis, improve disease prognostication, and provide a more robust marker of treatment response.

CHAPTER ONE

INTRODUCTION

1.1 Introduction

Lymphedema, Lymphatic system disorders, or elephantiasis, is a lymphatic system disorder caused by the accumulation of lymph which diminishes lymphatic return, resulting in swelling of one or more regions of the body, which is one of the common diseases worldwide. The lymphatic system consists of three sections, including liver, intestinal, and soft tissue lymphatics. Most lymphatic system diseases for primary or secondary causes arise from soft tissue. The lymphatic system covers all the body with multiple lymphatic-venous connections in different locations of the body. Thus, any physiological change or morphological blockade can result in the accumulation of the liquid, causing lymphedema. The central locations of lymph tissues are: Lymph nodes, spleen, bone marrow, adenoids and tonsils and thymus gland (Ohtani & Ohtani, 2012). (Figures 1.1 & 1.2)

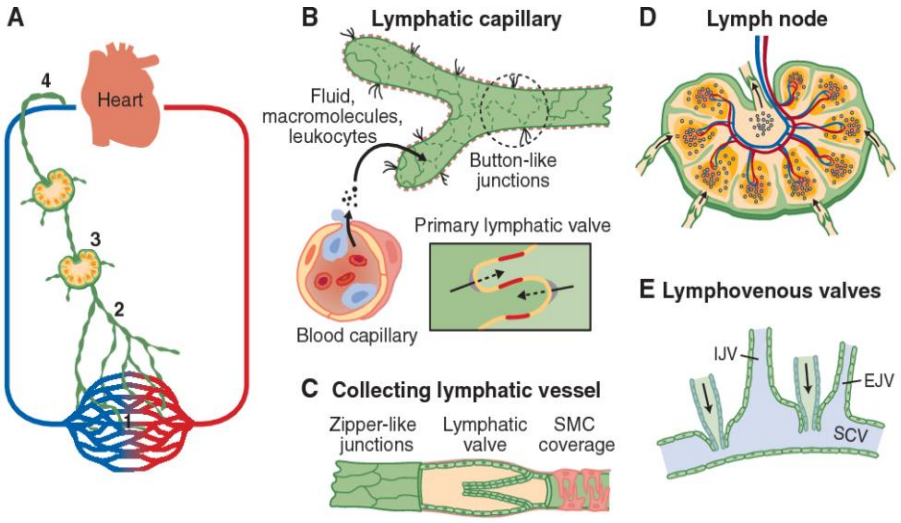

Figure 1.1: A: lymphatic system: B: lymphatic capillaries, C: collecting lymphatic vessels, and D: lymph nodes (Aspelund et al., 2016)

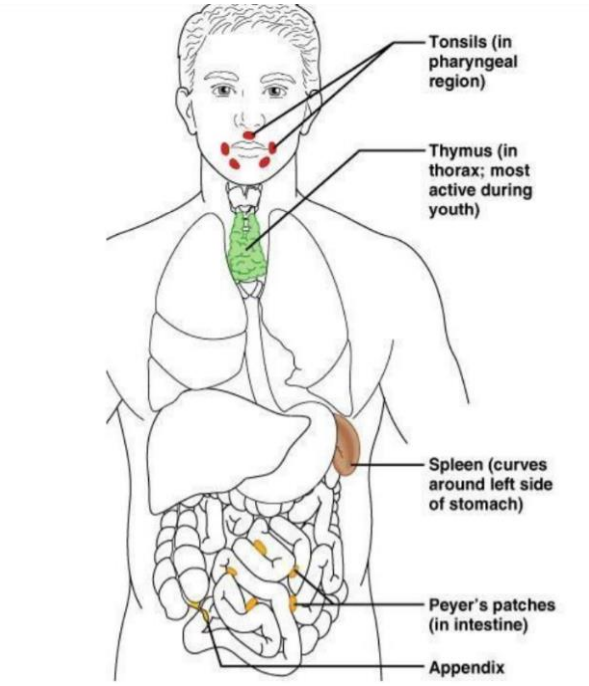

Figure 1.2: Lymphatic organs(Ohtani & Ohtani, 2012)

It is estimated that the incidence of this disease ranges between 140.0 to 250.0 million people globally (Young et al., 2016; Slavin et al., 2009). Lymphedema can affect all body parts and organs but more common is in specific organs such as lower limbs and upper limbs, with an incidence of 99% of total affected organs or regions (Arin et al., 2010).(Figure 1.3).

Figure 1.3: Lower limb lymphedema (Arin et al., 2010)

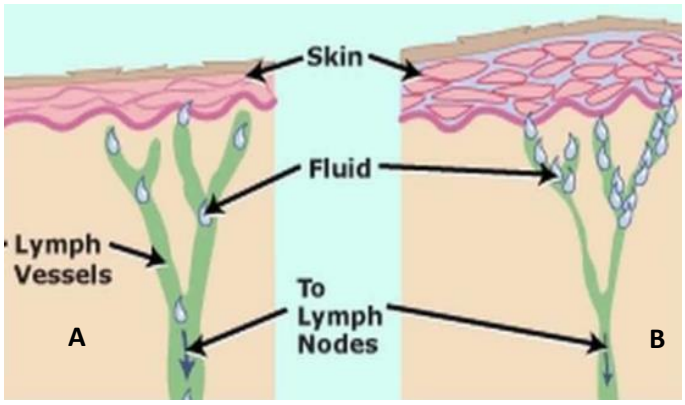

Figure 1.4: (A) Normal and (B) blocked lymph

Lymphedema may arise because of the lymphatic vessels or nodes which were either damaged or not formed correctly. (Figure 1.4: A&B)

Lymphedema can be classified into primary and secondary types according to the cause of the disease, whether it is congenital or acquired. (Figure 1.5).

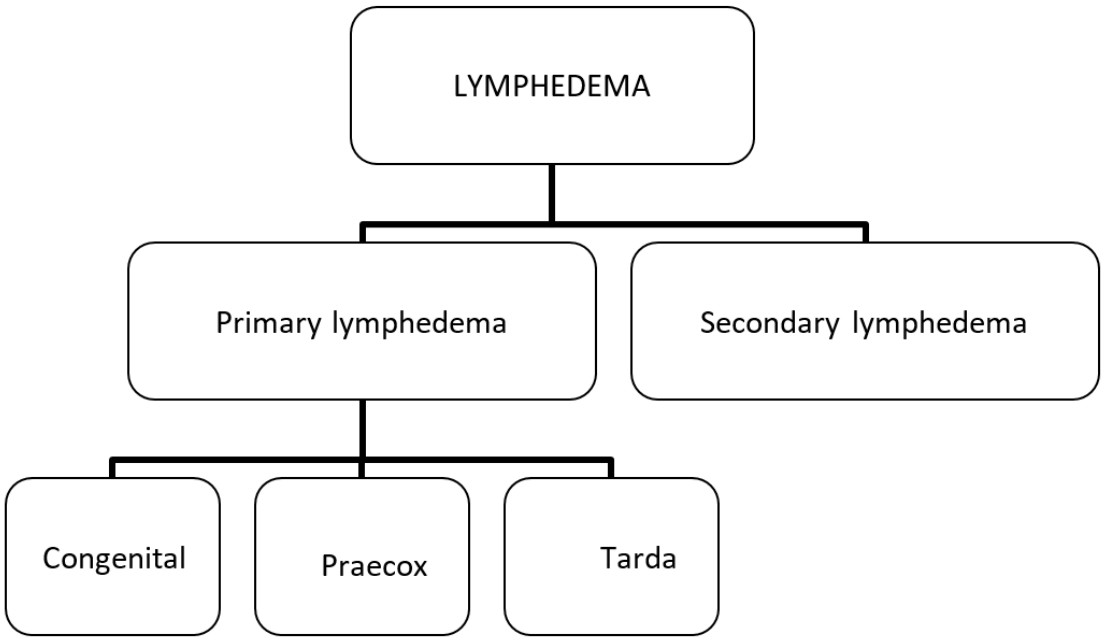

Figure 1.5: Types of lymphedema

Primary lymphedema is caused by congenital abnormalities, whereas secondary lymphedema is caused by infection, surgery, or radiation. The causes of lymphedema depend on the economic level or economic prosperity of a country. i.e., in developed countries such as the United States and Europe, the incidence is reported to have about 1.4 persons per 1000 persons, typically secondary to cancer treatment (8% after mastectomy, 38% after radiotherapy and axillary lymph node surgical removal) or cancer itself due to blockage of lymph vessels by metastasis. Thus, radiotherapy treatment is recommended to treat effects of lymph nodes in breast cancer rather than surgery to reduce the risk of lymphedema (Rutgers et al., 2013). While the leading cause of lymphedema in developing countries is an infection due to the parasite *Wuchereria bancrofti* (filariasis (Fig.1.6). Furthermore, it is estimated that almost 1.2 billion people are at the risk of contracting lymphatic filariasis in these countries. Currently, more than 120 million people are affected by lymphatic filariasis, another risk factor of lymphedema includes patient age, body mass index (BMI > 59 are high risk for spontaneous development of lower limb lymphedema, extremity infections, and trauma, chronic venous insufficiency.

Figure 1.6: Lymphatic filariasis endemic countries (approximately 18% of the population worldwide) (WHO, 2014)

1.1.1 Function of lymphatic system

The lymphatic system plays an essential role in human health. It is composed of an extensive network of vessels, nodes, and lymphatic organs. Diagnostic and therapeutic intervention with various imaging modalities are required to obtain an accurate diagnosis. Lymphedema is a lymphatic system disorder caused by the accumulation of lymph, which diminishes lymphatic return. Subsequently, there is an inflammation, hypertrophy of adipose tissue and finally, fibrosis.

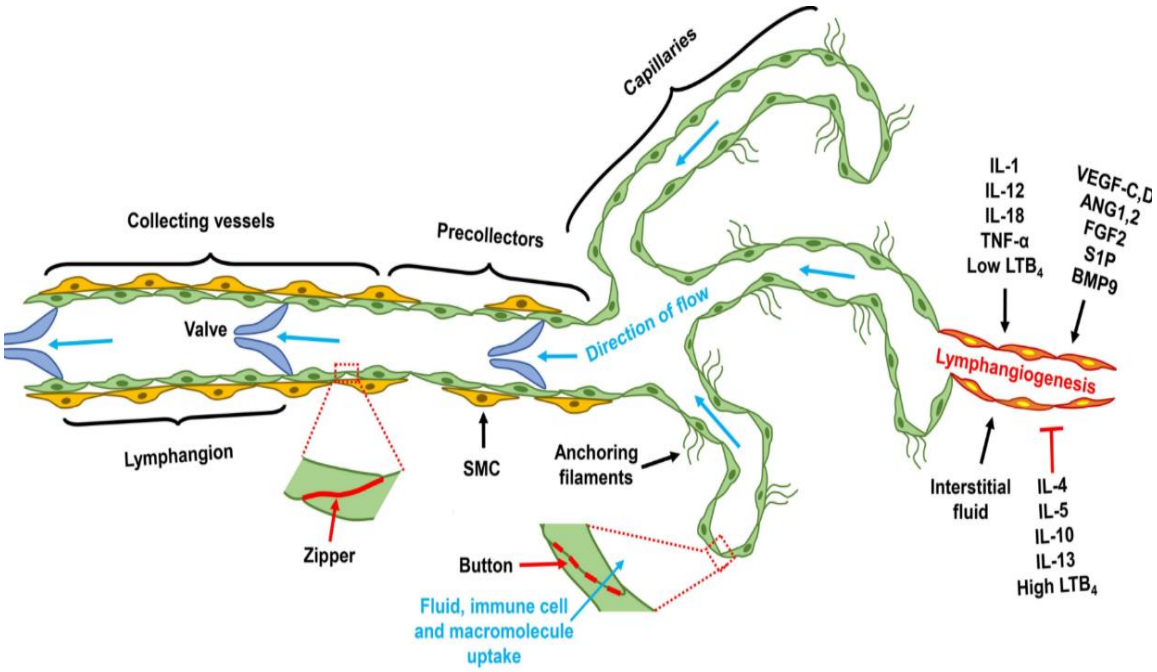

Figure 1.7: Lymphatic system vascular tree (Jiang et al., 2019)

Imaging of lymphatic systems (lymphangiography) was first introduced to clinical practice in 1951 using an oil-based contrast medium (Gough 1964). The procedure is invasive, complicated, and causing patient discomfort and is no longer performed due to its severe complications. Nuclear medicine scintigraphy of the lymph system (Lymphoscintigraphy (LS)) is frequently used to diagnose the system disorders. The main drawback of this technique is the low image resolution and the procedure accompanied by ionizing radiation for patients. Magnetic resonance lymphography (MRL) has been used to adequately examine the lymph vessels and identify their morphology (Carrasco et al., 2015). Different imaging techniques are used to diagnose lymphatic disorders, including lymphangiography, lymphoscintigraphy, computed tomography, MRL, PET/CT, and ultrasound imaging. However, all these techniques have different

limitations (Xiong et al., 2014). A contrast agent is used to create informative radiographic images by direct or indirect injection of contrast in the vessel. The direct injection may induce complications, which leads to the elimination of this technique. On the other hand, indirect injection is conducted by injecting the contrast interstitially. Various other techniques were developed to overcome the limitation of conventional ones. These techniques include scintigraphy, PET, SPECT, CT, and MRI.

Currently, MRI and PET MRI are the best imaging modalities to assess the pathology. MRI is usually used to alter relaxation time to enable accurate visualization of the anatomy and pathology (gadolinium compounds) (Xiong et al., 2014; Wu et al., 2011).

1.2 Lymph nodal Autotransplantation (LNT)

Lymph node transplantation (LNT) or Vascularized Lymph Node Transfer (VLNT) is the surgical treatment of lymphedema by transplanting lymph nodes from one part of your body to the limb with lymphedema (Huang et al., 2016). Currently, LNT is a useful microsurgical technique for re-vascularizing the lymph due to lymphangiogenic response (Aschen et al., 2014). LNT is used to decreases the side effect of lymphedemas, such as swelling, pain, and discomfort, without having significant side effects.

1.3 MR lymphographic Imaging

It is well documented that MRL provides useful anatomical and physiological data, thus enabling accurate diagnosis of the disease. It is reported that the procedure has 90% and 94 % sensitivity and specificity respectively (Mitsumori et al., 2016). Many commercial contrast mediums such as Gadodiamide compose of extracellular, water-soluble paramagnetic contrast agent with a gadolinium concentration of 0.5 mmol is normally administered IV at a recommended dose of 0.1 mmol per kilogram of body weight, which is equivalent to a dose of 0.2 mL/kg. For MR angiography, however, gadodiamide has been approved at doses up to three times the standard. Experimental animal models have shown merely minor tissue damage after non-IV injection or extravasation (Lohrmann et al., 2006; Cohan et al., 1991). Therefore, the agent offers an acceptable safety profile for intracutaneous administration.

Many authors reported the advantages of contrast studies and others attempt to acquire images without contrast medium. MRL consists of two sequences. The first is a 3D heavily T2-weighted sequence to depict the severity and extent of the lymphedema (Figure 1.3). The second is a fat-suppressed 3D spoiled gradient-echo sequence performed after the intra-cutaneous injection of an extracellular gadolinium-based MR contrast agent (Mitsumori et al., 2016). In addition to that, the authors reported that venous enhancement almost always

occurs which is one of the interpretative challenge in differentiating the enhancing lymphatic channels from superficial veins.

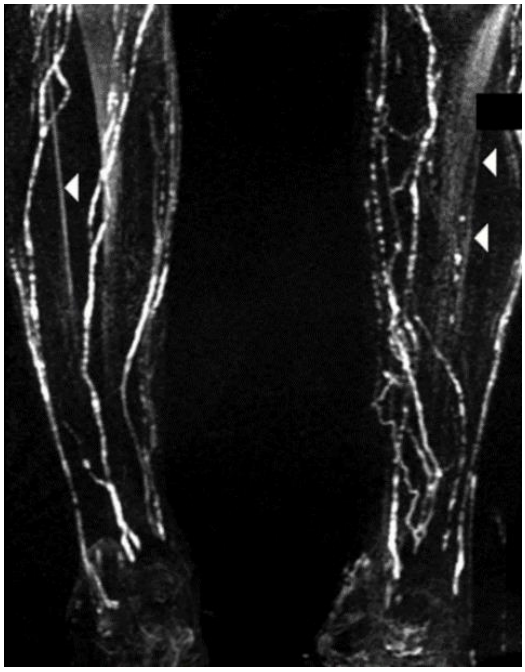

Figure 1.3: Gradientecho high-resolution MR lymphangiography sequence (arrows show enhanced veins) using gadodiamide injection (Lohrmann et al., 2005).

1.3.1 Non contrast MRL

Noncontrast MRL has substantial benefits as compared with other imaging techniques. In this context (Franconeri et al., 2020; Arrive et al., 2016) and Derhy et al. (2013) reported that Noncontrast MRL could be performed using heavily T2-weighted fast spin-echo sequences (to demonstrate the location of edema) with long T2 relaxation time. Derhy et al. (2013) stated that 3D MRL demonstrates retroperitoneal lymphatic aneurysmal dilatation. This dilatation exhibits a continuous spectrum of change from normal variants to lymphatic

aneurysmal dilatation of the system. The authors reported that this technique was useful in diagnosing any clinical condition. In another recent study, Arrivé et al. (2017) used non-contrast MRL for the evaluation of lymph node for secondary upper limb lymphedema. The authors used a free-breathing three-dimensional fast spin-echo sequence to evaluate axillary lymph node transplantation with non-contrast MRL in 17 patients with secondary upper limb lymphedema. The study recommended that non-contrast magnetic resonance lymphography was a scientific technique to analyse the lymph node results before and after the surgery. MR lymphography, with very heavily T2-weighted MR images, provides an excellent analysis of both lymphatic vessels and lymph nodes without contrast media. Kim et al. (2016) assessed the thoracic duct using coronal and axial images of heavily T2-weighted sequences without contrast medium. Nonenhanced MR lymphangiography is a safe and effective method for imaging the central lymphatic system. It contributes to differential diagnosis and is appropriate to assess preoperative evaluation of pathologic lymphatic problems. The main limitation of non-contrast T2 imaging is that it does not provide information about lymphatic flow and the lack of a contrast agent makes it challenging to visualize small lymphatic ducts (Figure 1.4). Consequently, its use in diagnostic and interventional lymphangiography is limited (Dori 2016).

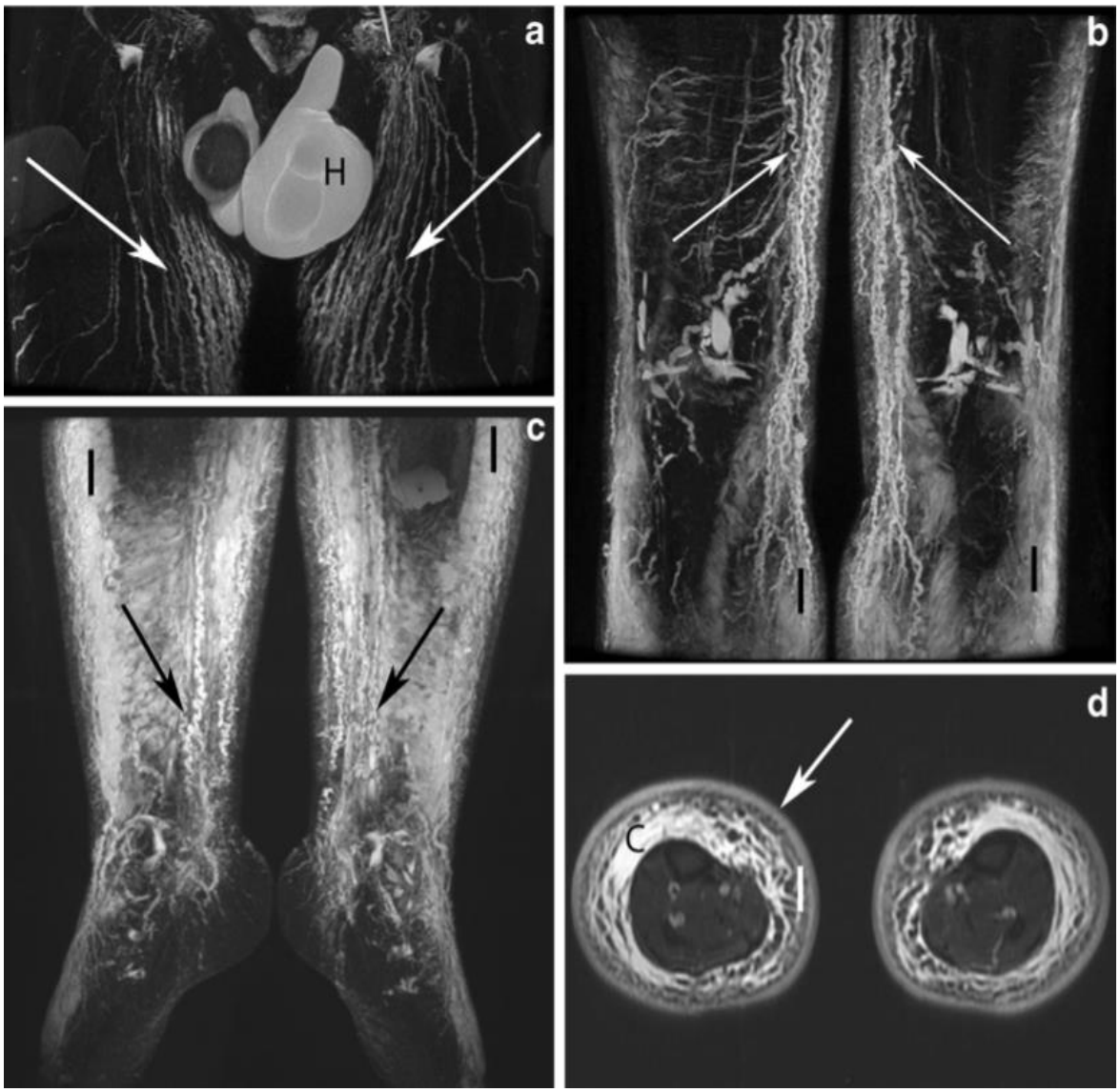

Figure 1.4: Non-contrast MRL for 54 old male patients shows (a) dilated lymphatic iliac and inguinal trunks (b,c) Dilated lymphatic vessels (d) Water IDEAL T2 FSE image (Arrivé et al., 2017).

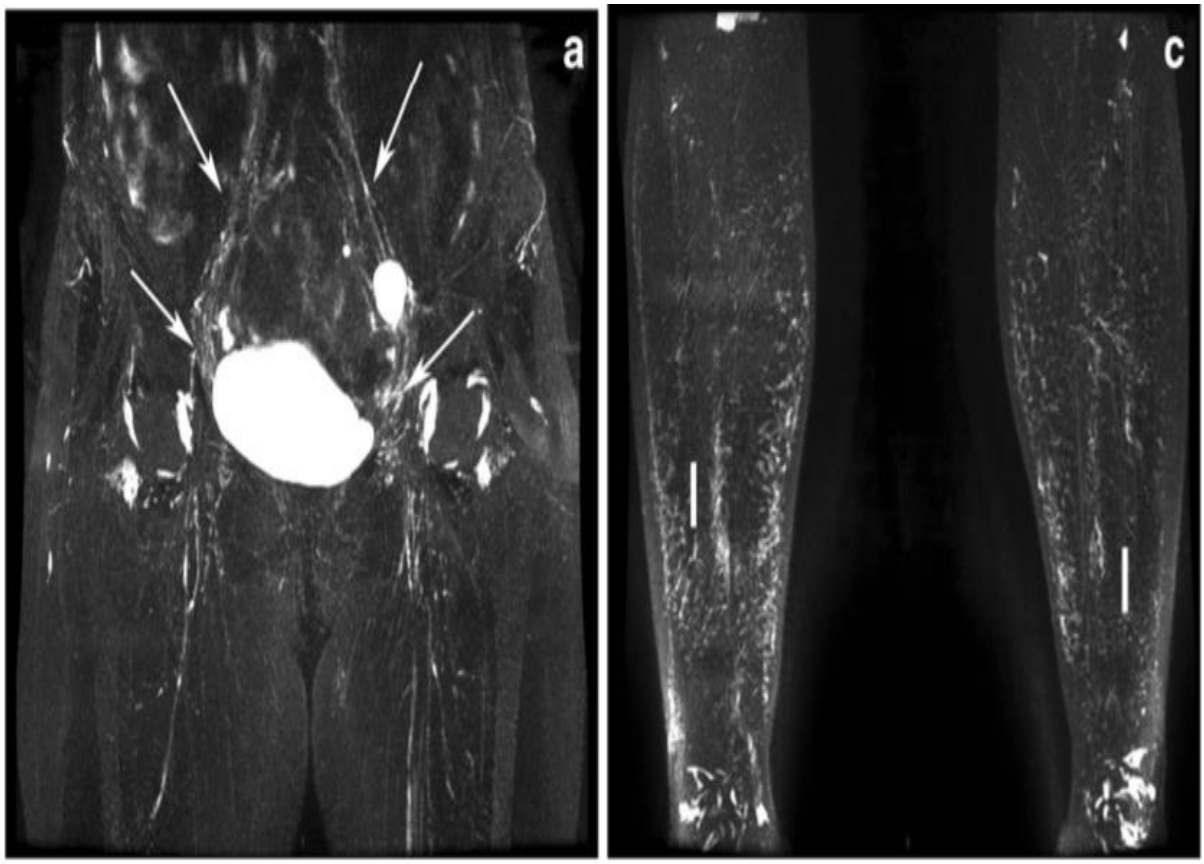

Figure.1.5: Non- contrast MRL for 52 female patients with lower limb lymphedema shows (a) a normal pattern of iliac and inguinal lymphatic trunks (arrows) at both sides and (b,c) a lower levels (Arrivé et al., 2017).

1.4. Exposure to ionizing Radiation during Lymphography

Computed tomography (CT) and single-photon emission computed tomography (SPECT) for medical diagnostic imaging are increasing for differential diagnosis of lymphedema. Patients were exposed to a significant-high radiation dose range between 2.5 up to 30 mSv from CT procedures (ICRP 2007). Rehani et al. (2020) reported that more than 2.5 million patients received an effective dose above 100 mSv due to repetitive radiation exposure.

The incidence of lymphedema is increasing due to an increase in cancer incidence and the survival rate of cancer treatment advances. Radiation-induced cancer due to CT imaging contributes to 2.0 % of current cancer incidence in the United States (Brenner et al., 2007). The benefit of using justified, as low as reasonable, radiation doses exceed the projected radiogenic risks. However, still the patients are exposed to less optimized CT procedures.

1.4 Statement of the Problem

Lymphedema is a significant disorder of the lymphatic system that occurs primarily due to lymphatic system disorders or secondary lymphedema caused by radiation therapy involving lymph nodes or surgical operation dissection. Traditional techniques for diagnosing lymphedema include pedal lymphangiography (PL), which is replaced by intraoral lymphangiography. It is an invasive procedure and requires an extended time to accomplish the procedure (Nadolski and Itkin 2013). In intradermal pedal lymphoscintigraphy, the use of SPECT CT is essential to overcome the limitation of limited spatial resolution. The radiation dose to patients and staff is one of the main concerns of the procedure. MR lymphangiography is used by injection contrast medium (gadolinium) subcutaneously or intradermally. The drawback of this procedure does not provide sufficient findings due to the delusion of the contrast agent. Dynamic contrast-enhanced MR lymphangiography is currently used to provide

excellent spatial resolution and dynamic flow of the lymph. This procedure also has limitations regarding the imaging of traumatic patients and the side effects of using contrast media for patients with kidney function disorders. Thus, the only option available is to develop a protocol for lymphedema without contrast agents to reduce the contraindication of the procedure and extract diagnostic information without contrast medium. In addition to that, no previous study, to my knowledge was conducted for lymphedema evaluation without contrast medium pre and post-operative.

1.5 Statement of the purpose

To evaluate the role of MR-lymphographic for the assessment of lymphedema before and after lymph node self-transplantation.

1.5.1 Specific objectives.

1. To update the general database: especially patients Pre and Post lymph nodal autotransplantation.

2. To Measure the Lymphedema for every single exam according to our score

3. To create the database with the new data

4. To find clinical data for each single patient

5. To Evaluate the patients' risk from SPECT/CT and CT imaging resulted from ionizing radiation exposure during lymphedema management

1.6 Thesis Outlines

This research is concerned with non-contrast MR-Lymphography which is a new tool for evaluation of lymphedema pre and post-lymph nodal autotransplantation. Hence, the thesis is divided into five chapters according to the following sequence:

Chapter one is the introduction of the thesis. In this chapter, the author provides the context of the study, rationale, and significance of the problem. The Statement of the purpose is clearly described with reasonable background, thesis outline, and thesis outcome.

Chapter two contains the theoretical background of the study, along with the review of previous literature.

Chapter three designates the methods and materials used in this thesis, patient population, and statistical analysis.

Chapter four presents the results of the thesis, and finally,

Chapter five contains the discussion, conclusion, and recommendations of the thesis and presents suggestions for future work.

1.7 Thesis outcome:

1.7.1. Publications:

1. **Abdullah Almujally** and Fabrizio Calliada. Review of Non-Contrast MR-Lymphography Techniques and Findings: Challenges and Opportunities. Open Journal of Radiology. 10 (2), 1-10, 2020

2. **Abdullah Almujally** and Fabrizio Calliada. Evaluation of magnetic resonance lymphangiography for patient's undergoing pre and post microsurgery. Medical Science Journal. 24 (104), 2267-2272, 2020

3. **Abdullah Almujally**, Sulieman A., Fabrizio Calliada. Patients Radiation Risks from Computed Tomography. Lymphography. Journal of Clinical Imaging Science. 2020, 10,46,1-5.
4. **Abdullah Almujally**, Sulieman A.,Hasan Salah, Bandar Alanazi, Fabrizio Calliada. Patient dosimetry in SPECT/CT lymphoscintigraphy examinations. Journal of Research in Medical and Dental Science. 8 (5), 97-100, 2020.

1.7.2. Conference Presentations

1. **Abdullah Almujally**, Sulieman A., Fabrizio Calliada. Patients Radiation Risks from Computed Tomography Lymphography. The International Conference on Radiation Medicine (ICRM2020), 9-13 February, 2020.

CHAPTER TWO

THEORETICAL BACKGROUND

2.1 Theoretical Background

This chapter provides the necessary information to understand the concept of MRI imaging and assessment of previous studies. Therefore, I will provide background regarding MRI systems and to covers the MR lymphography with contrast and without contrast.

2.1 MR systems

Magnetic resonance imaging (MRI), a chemically sensitive in-vivo imaging technique, is a medical noninvasive imaging technique that produces three dimensional (3D) images of the human body using a magnet and magnetic characteristics of human body tissues and organs. Since its introduction to clinical use in 1977 (Damadian et al., 1977), MRI systems developed rapidly to meet the requirements of high diagnostic yield with minimal discomfort and short time. Different MR systems configurations are available (Figures.2.1 &2.2). MRI technology is based on the use of powerful magnet: electrical (superconductive) or resistive or permanent. The radiofrequency signals to induce body tissues to re-emit the absorbed radiofrequency. Thus, the use of metals or ferromagnetic materials must be eliminated in manufacturing the MRI systems to avoid signal interferences and artifacts. The main components of the MRI system are: (i) Radio Frequency (RF) Transmitter, (ii) Main Magnet 0.2 to

3.0-tesla (Resistive, Permanent, or Superconducting), (iii) RF coils, (iv) 3 Gradient Magnets 18 to 27-millitesla or 180 to 270 gauss, (v) RF amplifier

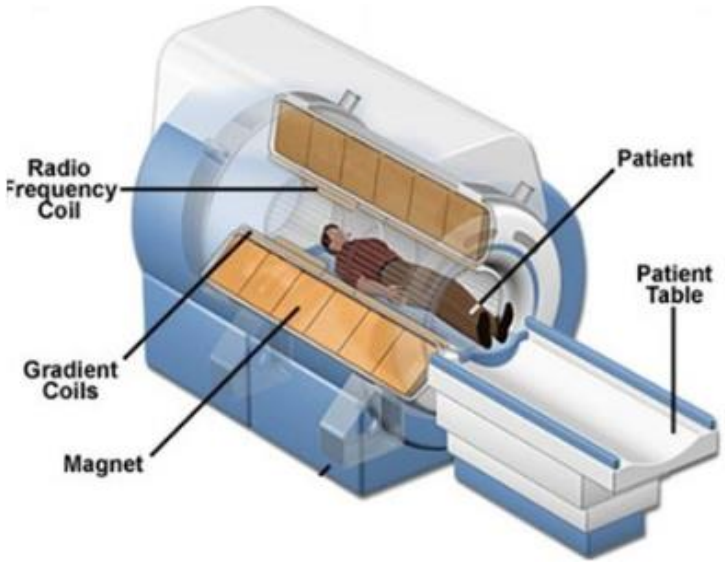

Figure 2.1: MRI system configuration (Coyne, 2012)

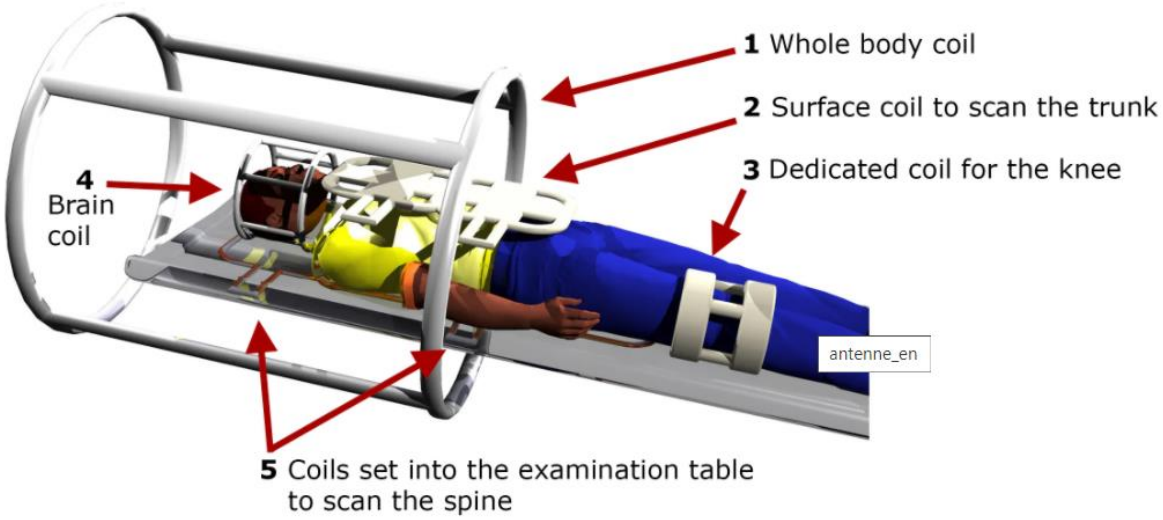

Figure 2.2: MRI radiofrequency system component (IMAIOS,2020)

2.1 MRI Magnet

Magnets are one of the essential components in MRI technology. These are used to create a strong magnetic field that ranged from 0.2 to 7.0 Tesla. Superconducting magnet, which is made up of coils through which an electrical current creates a magnetic field, is preferred since its first introduction using NbTi alloy in the 1960s due to its numerous advantages (Cosmus and Parizh, 2011).

2.1.1 Permanent magnet:

The permanent magnet delivers a magnetic field, which is always on at full strength and, therefore, does not require electricity. The cost to run the machine is low due to the constant magnetic force. However, the major drawback of these magnets is the weight concerning the magnetic field they produce. The permanent-magnet MRI systems are heavyweight. Their installation cost is rather high, but the maintenance cost is low. The low-field magnets typically have relatively poor uniformity and stability. Poor uniformity results in poor image quality, although it might be adequate for some applications. With few exceptions, MRI systems with a central field strength higher than 0.35 tesla use superconducting coils. MRI with superconducting magnets accounts for more than 75% of the installed MRI base. Advantages of superconducting MRI systems include, but are not limited to, better performance, higher signal-to-noise ratio

as a result of higher field, higher resolution, and lower lifecycle cost (Davies 2000, Lvovsky 2005). MRI uses the majority of superconducting materials produced worldwide. MRI magnets use about 60% of all superconducting wire (including copper), and about 40% of the NbTi alloy (Cosmus and Parizh, 2011). The higher fraction of conductor is since MRI magnets use conductors with a high copper; a typical MRI conductor contains 80 to 90 percent volume of copper and only 10% to 20% NbTi.

The advantages of permanent magnet include no use of cryogens, thus meagre running costs. The disadvantages include only low field <0.5T, usually very heavy magnets are sensitive to temperature changes, vertical Bo involves new coil designs (Figure 2.3)

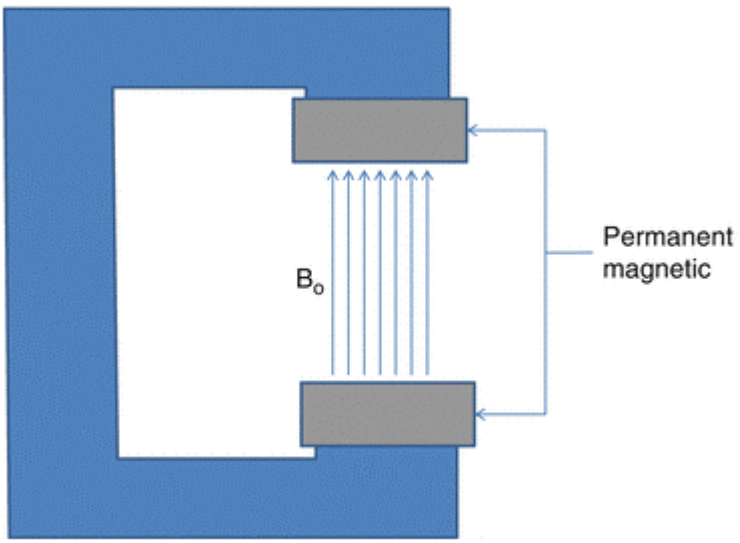

Figure 2.3: Permeant magnet

2.1.2 Superconducting magnet

An installed MRI base after 30 years of commercial production reaches a state of maturity. The healthcare industry demands for high efficiency, low cost, and reliable systems resulted in technically-challenging, well-integrated magnet designs, are reproducible in volume production.

In 2008, the total installed base of superconducting MRI systems was about 26,500 units vs. 14,600 systems in 2002. More than 2,500 superconducting MRI scanners are produced annually. The field strength depends on the shape. There are several types of superconducting MRI magnets. Thousands of commercial whole-body systems of 1.5 Teslas and 3 Teslas are produced worldwide. The very-high field 4.0 T to 21.1 T units are evaluated at research sites and are for investigational use only. A unique 11.7-tesla scanner is being built to be installed in Saclay, France (Vedrine et al., 2010).

Recently, in 2017, the European Union and Food and Drug Administration (FDA) in the USA approved the use of the 7 Tesla MRI scan in August clinical imaging.

A higher image resolution can be obtained by using the 7 T MRI scanner in clinical use, thus it is useful for the diagnosis of the brain and knee joint pathologies.

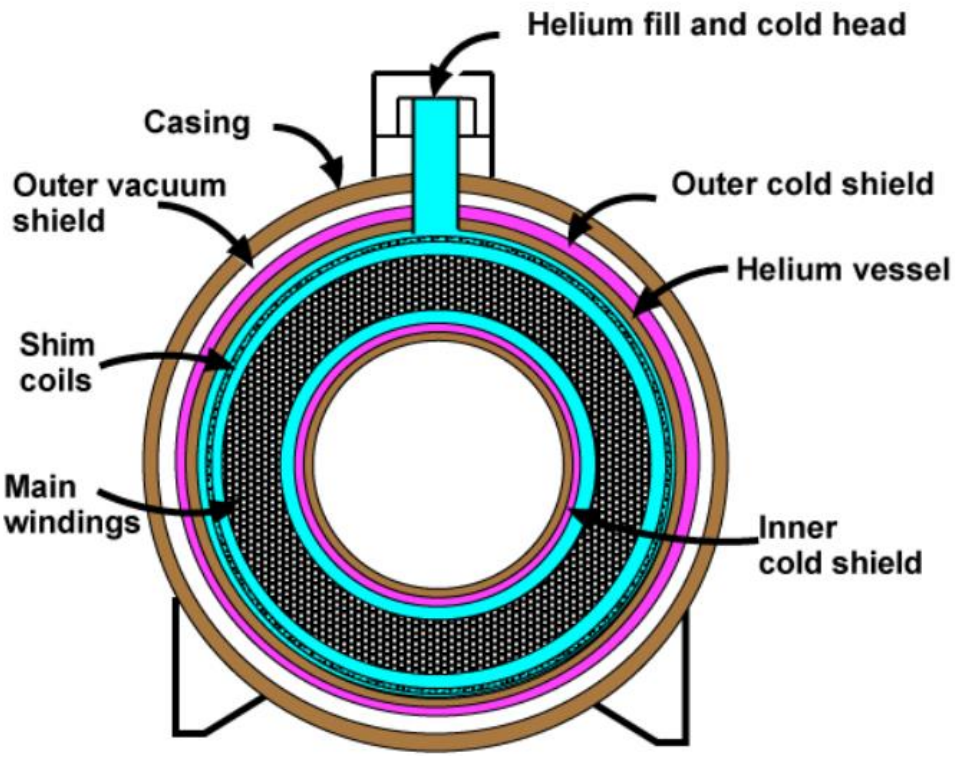

Figure 2.1: Cross-section of superconducting magnet

During the last decade, the lower-field superconducting 0.5 T and 1.0 T cylindrical scanners practically went out of production. Their marginally-lower cost was insufficient to outweigh the commercial 1.5 T systems' advantages in faster patient throughput and better image quality. Until the late 1980s, the lower-field systems dominated the MRI market. In year 2000, approximately 600 low-field systems were produced, representing greater that 20% of the market segment. By the year 2005, their production was practically stopped.

The 1.5-tesla units represent the majority of scanners produced in recent years (Figure 2.1). The 1.5 T systems are a good compromise between performance, patient comfort, ease of sitting in a hospital environment, optimized installation,

and the life-cycle cost of the equipment. After several years of research use, the 3-tesla whole-body scanners from General Electric, Philips, and Siemens entered the marketplace in the early 2000s. Initially, the commercial 3.0 T scanners were rather large and heavy, weighing 10,000 kg or more. The latest 3-tesla scanners have a significantly lower weight. Their dimensions and uniformity volume are now similar to 1.5-tesla scanners. The Philips' Achieva 3 T weighs only 5,600 kg (including cryogens).

About thirty higher-field whole-body 7 tesla to 9.4 tesla systems are installed at luminary sites around the world, usually in the university hospitals. Initially, these scanners were used solely for brain imaging that require a relatively small image area with high uniformity. A few research centres are extending imaging to cardiac, prostate, breast, extremity, and other areas, with the ultimate goal of expanding the range of applications beyond high resolution anatomic and functional brain imaging. The high-field magnets are highly customized depending on the image volume, bore size and the type of shielding etc. The length of 7-tesla magnets varies from 2.6 m to 3.5 m. The whole-body 7 T systems provided by Philips to several research sites had a magnet that weighed 32 tons and had steel shielding options of 218 tons and 406 tons (Agilent Technologies build the magnet). A similar Siemens 7 T scanner weighed 32 tons and required 250 tons of wall shielding (Damadian et al., 1977). The last decade

shows how definitions may change. In the 1980s, the 1.0 T MRI units were called high-field. In the 1990s, the 1.5 T systems were called high field 'while 3 T MRI were ultra-high field. Today, 1.0 T cylindrical magnet is a low field unit, 1.5 T is the standard field, although 1.0 T Open magnet is considered a high-field unit for that geometry. The 3 T MRI are moderate field units, and 7 T higher-field MRI are called ultra-high field. In the future, advances in magnet technology could rename the 3 T MRI to the standard field.

More than 95% of superconducting MRI magnets have a standard cylindrical shape (Figure 2. 4). It allows minimization of the stray field, compact dimensions, and low cost. This configuration permits mobile configuration that may move from location to location while at a nominal field, thus minimizing the setup time.

Cylindrical MRI systems have a known but accepted limitation: the narrow patient bore of typically 60-cm diameter and >100 cm length. This tunnel creates several issues:

1. Obese patients may not fit into the tunnel.
2. A claustrophobic effect causes certain patients to reject the procedure creating a financial loss for the image center and diagnostic loss for the patient.
3. It restricts interventional medical procedures.

More recently, the patient bore has become a limiting factor for specific image-guided medical procedures. The image-guided medical ablation is an example of such a procedure. It requires patient access to an open MRI with a center field of at least 0.5 T. This procedure uses 3D MRI images to facilitate biopsy or treatment of tumors, e.g., liver cancer (Davies, 2000).

Open MRI is limited to a field of about 1 T. The open magnet uniformity volume is often smaller than in 1.5 T and 3 T cylindrical scanners. This may result in lower image quality and longer scanning time. The stray field may be higher than in 1.5-tesla scanners.

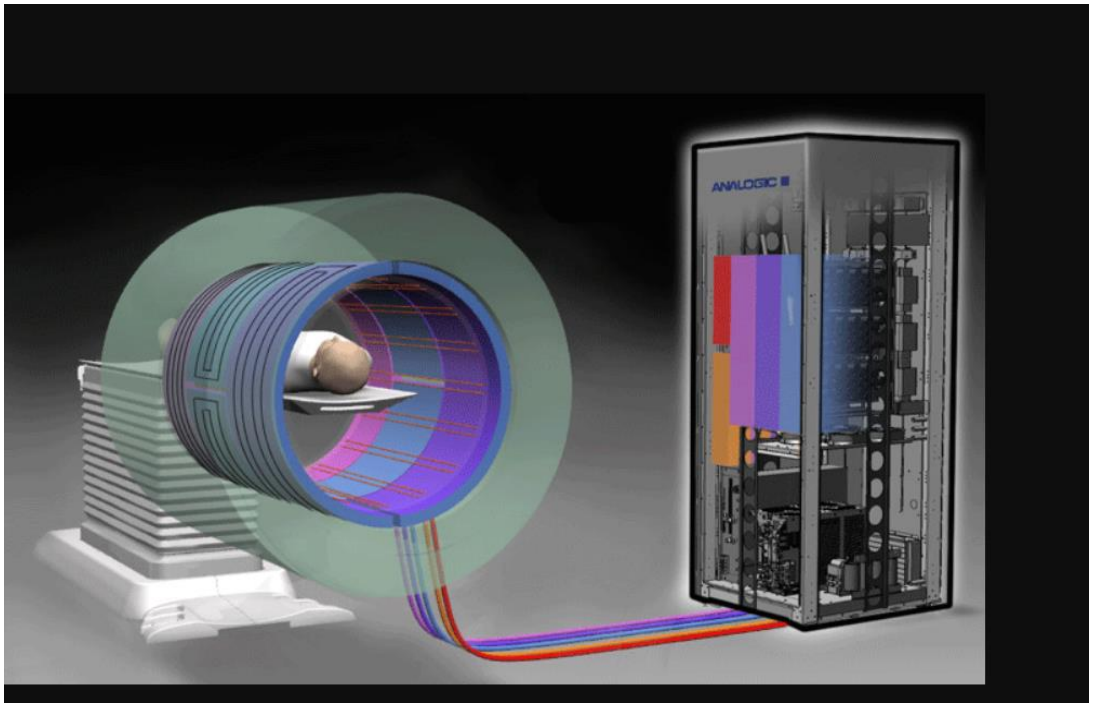

Figure 2.4: Schematic illustration of the MRI system for the three cardinal directions: x, y, and z, where the main components are indicated. (Coyne, 2012).

2.2MR systems

An MRI sequence is an ordered combination of RF and gradient pulses designed to acquire the data to form the image. In this chapter, the researcher will describe the basic gradient echo, spin-echo, and inversion recovery sequences used in MRI. The data to create an MR image is obtained in a series of steps. First, the tissue magnetization is excited using an RF pulse in the presence of a slice select gradient. The other two essential elements of the sequence are phase encoding and frequency encoding/readout, which are required to localize the protons spatially in the other two dimensions. Finally, after the data has been collected, the process is repeated for a series of phase encoding steps. The MRI sequence parameters are chosen to best suit the particular clinical application. The parameters affecting soft tissue contrast are described, and advanced sequences such as STIR, FLAIR, FISP, and FLASH are briefly introduced at the end of the chapter MRL sequences

2.3 MRL imaging protocols

The MRL technique could vary slightly depending on the MR equipment and the anatomical site of the investigation but can be outlined as follows;

2.3.1 MR Equipment

The preferred MR equipment includes a 1.5-Tesla or more MR unit. In our experience, all MR examinations were performed by a General Electric

Healthcare Signa TwinSpeed HDxt, with a maximum gradient strength value of 23 mT/m and a slew rate of 80 mT/m/ms (software release 15.0_0947A). A multielement body coil is fundamental for this type of examination. For our purposes, we used a receiving phased-array peripheral vascular coil to study the lower extremities (Flow 7000 phased-array peripheral vascular, USA Instruments) and an 8-channel body array coil for the upper extremities with both a significant anatomical coverage and a good signal-to-noise ratio.

2.3.2. Positioning of the Patient

Patients should be fully informed about the procedure to confirm their complete collaboration. Positioning varies depending on the anatomical site of the investigation.

2.3.2.1. Lower Limb: The patient is placed in the supine position, feet first, with both legs on a ramp pillow so that the lower extremity is parallel to the main magnetic field and near the most homogeneous area of B0. According to the height of the patient, three or four stations are examined to cover the following anatomical regions:

1. The lower leg inferior segment and foot region (feet region)
2. The lower leg superior segment and upper leg inferior segment, including the knee region (calf region)

3. The middle-upper leg and the proximal upper leg including inguinal region (thigh region and pelvic region)

The toes of both feet emerge from the coil's holes and are easily accessible for the injection of the contrast medium (Figure 2.2).

2.3.3 Contrast Medium Administration

A mixture of the standard dose (0.1 mmol/kg body weight) of a paramagnetic contrast medium and 0.5 mL of lidocaine 1% for local anaesthesia is injected subcutaneously/intradermally. For our purposes, the contrast medium used was gadobenate dimeglumine (Gd-BOPTA, Multihance, Bracco Imaging, Milan, Italy). Since experimental animal models have only shown minor tissue damage after intracutaneous injection or extravasation, a gadolinium medium offers an acceptable safety profile for intracutaneous administration at the recommended dose, even if it is still considered as an off-label use (Arrivé et al., 2017; Mitsumori et al., 2016; Derhy et al., 2013).

Lidocaine 1% is administered with the contrast medium also to alleviate pain during the injection. Generally, no complications are observed after the examination, particularly during or after intracutaneous injection of Gd-BOPTA.

2.4. MR Parameters and Sequences

The imaging protocol generally consists of a heavily T2-weighted sequence to evaluate the extent and distribution of the lymphedema and of a 3D fast spoiled

gradient-echo T1-weighted sequence with a fat-saturation technique for the lymphatic visualization (Wu et al., 2016, Kim et al., 2011). In our experience, we performed a 3D steady-state free precession (SSFP) balanced electrocardiography- (ECG-) triggered sequence (FIESTA, GE) with fat spectral saturation (SPECtral inversion at lipid, SPECIAL, GE) instead of a heavily T2-weighted sequence in order to obtain a good visualization of both the venous system and the distribution of the lymphedema within the same sequence and at the same time. The study was conducted in three steps: (1) a survey and a mandatory calibration were performed for all stations, three or four for the lower extremity (foot-ankle-calf, calf-knee, and thigh-hip) and two or three for the upper extremity (hand-wrist-forearm, elbow-arm-shoulder). Before injection of the contrast medium, a coronal 3D SSFP-balanced ECG-triggered sequence with fat spectral saturation (Spectral inversion at lipid, Special, GE) was acquired. The ECG-trigger was acquired with a peripheral gating (PG, GE). A time delay was set for a systolic phase acquisition to obtain non-contrast-enhanced venograms and clear images for the visualization of lymphedema. We then performed a pre-contrast coronal 3D spoiled gradient-recalled echo T1-weighted sequence with Spectral inversion at lipid (FSPGR with SPECIAL, GE) in all stations in order to increase contrast sensitivity and then subtracted this pre-contrast sequence ("mask") from subsequent postcontrast images; (Xiong L. et

al. 2014) the patient is brought out of the bore and instructed not to move. Two radiologists begin to inject the contrast medium simultaneously (one for each extremity), using a 28G thin needle inserted consecutively into the dorsal interdigital spaces of both the extremities; (Wu et al. 2011) the first station is repeated 5, 20, and 35 minutes after the injection of the contrast medium. The other one/two stations are examined in sequence after the first station at each fixed time (5, 20, and 35 minutes). Each 3D SSFP-balanced sequence lasts about 3 minutes. Each 3D spoiled gradient-recalled echo T1-weighted sequence lasts nearly 3 minutes and 50 seconds, with a total average examination time of 1 hour and 15 minutes for the lower limb (3 minutes × 3/4 anatomical regions/stations and 3 minutes and 50 seconds × 3/4 anatomical regions/stations × four times [time of 0, 5, 20, and 35 minutes]) and 50 minutes for the upper limb. The technical parameters used for the suggested sequences are shown in Table 2.1.

2.5 MRI contrast mediums

Since the first ferric chloride was used in MRI as a contrast medium in MRI imaging in 1981. Recently, many contrast mediums have been developed for use in clinical practice, and some of them were withdrawn as a result of safety concerns. The MRI contrast mediums discovered to date may be classified into various groups according to several criteria: chemical composition, the presence

of metal atoms, and the route of administration, magnetic properties, and the effect on the image, biodistribution and further applications. As a result, there are variations in the clinical implications, mechanisms of action, safety, pharmacokinetics, and pharmacodynamics of the contrast media. Currently, newer and safer MRI mediums capable of targeting organs, sites of inflammation, and specific tumors are under investigation to develop contrast mediums with higher disease specificity.

MRI contrast media are classified according to the following specific features:

1. The chemical composition including the presence or absence of metal atoms
2. The route of administration
3. Magnetic properties
4. Effects on the MR image
5. Biodistribution and imaging applications.

The majority of these mediums are either paramagnetic ion complexes or superparamagnetic magnetite particles that contain lanthanide elements such as gadolinium (Gd^{3+}) or transition metal manganese (Mn^{2+}).

2.5.1 Effects of MR contrast media

The effects of MR contrast include:

1. Shorten the T1 or T2 relaxation time, thereby causing increased signal intensity on T1-weighted images or

2. Reduced signal intensity on T2-weighted images. Most paramagnetic contrast mediums are positive mediums.

These mediums shorten the T1, so the enhanced parts appear bright on T1-weighted images. Dysprosium, superparamagnetic mediums, and ferromagnetic mediums are negative contrast mediums. The enhanced parts appear darker on T2-weighted images. MRI contrast mediums that incorporate chelating mediums reduce storage in the human body, enhance excretion, and reduce toxicity. MRI contrast mediums may be administered orally or intravenously. According to biodistribution and applications, MRI contrast mediums may be categorized into three types: extracellular fluid, blood pool, and target/organ-specific mediums. Several contrast mediums have been developed to distinguish liver pathologies selectively. Some mediums are also capable of targeting other organs, inflammation as well as specific tumors.

Table 2.1: Contrast media for oral administration (Xiao et al., 2016)

Short name	Generic name	Trade name	Enhancement
Gd-DTPAa	Gadopentate dimeglumine	Magnevist Enteral	Positive
a	Ferric amonium citrate	Ferriseltz	Positive
a	Manganese chloride	LumenHance	Positive
a	Gadolinium-loaded zeolite	Gadolite	Positive
OMP-a	Ferristene (MPIO)	Abdoscan	Negative
AMI-121-b	Ferumoxsil (MPIO)	Lumirem/GastroMARK	Negative
PFOB-b	Perfluoro-octylbromide	Immedium GI	Negative

a Mediums available for clinical application

b mediums withdrawn from market. MPIO, micron size iron oxide particles.

Table 2.2: contrast media extracellular fluid (ECF) space mediums.

Short name	Generic name	Trade name	Enhancement and physiochemical effects
Gd-DTPA-a	Gadopentate dimeglumine	Magnevist	Positive-ionic-linear
Gd-DOTA-a	Gadoterate meglumine	Dotarem, Artirem	Positive-ionic-macrocyclic
Gd-DTPA-BMA-a	Gadodiamide injection	Omniscan	Positive-nonionic-linear
Gd-HP-DO3A-a	Gadoteridol injection	ProHance	Positive-nonionic-macrocylic
Gd-DTPA-BMEA-a	Gadoversetamide	OptiMARK	Positive-nonionic-linear
Gd-DO3A-butrol-a	Gadobutrol	Gadovist	Positive-nonionic-macrocyclic
Gd-BOPTA-a	Gadobenate dimeglumine	MultiHance	Positive-ionic-linear

a Mediums available for clinical application. ECF, extracellular fluid; Gd-DTPA, gadolinium (III) diethylene triamine pentaacetate; Gd-DOTA, gadoterate dotarem; Gd-DTPA-BMA, gadolinium 3-diethylenetriamine pentaacetate-bis(methylamide) ((Xiao et al., 2016)

2.6. MRI contrast media side effects

MRI contrast media side effects fall into three categories Minor, mild and severe side effects according to the patients and contrast volume and contrast type. These effects include:

2.6.1. Minor effects:

1. Nausea
2. Vomiting
3. Sneezing
4. Urticaria
5. Pain in arm
6. Sensation of warmness

2.6.2. Moderate effects:

Persistent

1. Headache
2. Severe urticaria and bronchospasm
3. Wheezes abdominal cramps
4. Hypotension with bradycardia
5. Severe vomiting

2.6.3. Severe and life-threatening

1. Laryngeal edema

2. Angioneurotic edema

3. Hypotension with tachycardia

4. Anaphylaxis (2nd) severe

5. Seizure

6. Cardiac arrest

7. Pulmonary edema

8. Unconsciousness / no response / pulseless /cardiopulmonary collapse and death

2.7 Previous Studies

The lymphatic system plays a vital role in human health. It is composed of an extensive network of vessels, nodes, and lymphatic organs. Diagnostic and therapeutic intervention with various imaging modalities is required to obtain an accurate diagnosis. Lymphedema is a lymphatic system disorder caused by the accumulation of lymph, which diminishes lymphatic return. Subsequently, there is inflammation, hypertrophy of adipose tissue, and finally, fibrosis. Imaging of lymphatic systems (lymphangiography) was first introduced to clinical practice in 1951 using an oil-based contrast medium (Gough 1964). The procedure is invasive, complicated, and causing patient discomfort and is no

longer performed due to its severe complications. Nuclear medicine scintigraphy of the lymph system (Lymphoscintigraphy (LS)) is frequently used for the diagnosis of the system disorders. The main drawback of this technique is the low image resolution and the procedure accompanied by ionizing radiation for patients. More recently, magnetic resonance lymphography (MRL) has been used to adequately examine the lymph vessels and identify their morphology (Carrasco et al., 2015). Different imaging techniques are used to diagnose lymphatic disorders (lymphangiography, lymphoscintigraphy, computed tomography, MRL, PET/CT, and ultrasound imaging). However, all these techniques have different limitations (Xiong et al., 2014). A contrast medium is used to create informative radiographic images by direct or indirect injection of contrast in the vessel. The direct injection may induce complications, which lead to the elimination of this technique. On the other hand, the indirect injection was conducted by injecting the contrast interstitially. Various other techniques were developed to overcome the limitation of conventional ones. These techniques include scintigraphy, PET, SPECT, CT, and MRI.

Currently, MRI and PET MRI are the best imaging modalities to assess the pathology. Contrast MRI is usually used to alter relaxation time to enable accurate visualization of the anatomy and pathology (gadolinium compounds) (Xiong et al., 2014, Wu et al., 2011).

2.7.1 MR lymphographic Imaging

MR imaging is useful technique for lymphatic system imaging and lymph-node staging approaches are based on size of lymph nodes in a radiographic image acquired by MR imaging or computed tomography (CT) images. The main drawback of the MRL technique is the low sensitivity (Williams et al., 2001; Yang et al., 2000). Lately, monocristalline iron oxide nanoparticles contrast media was developed that appeared to have been accumulated in macrophages after IV administration. Accordingly, on T2- weighted MR images, these agents cause signal loss in normal lymph nodes (Herborn et al., 2002; Weissleder et al., 1994; Rety et al., 2000). This selective enhancement allows some degree of differentiation between normal and tumor-bearing lymph nodes, especially in the pelvis. Problems associated with the visualization of negative enhancement—particularly in lymph nodes with partial tumor infiltration—appear to limit the clinical impact of this technique (Bellin et al., 1998). A more selective enhancement of the lymphatic system can be achieved with interstitial MR lymphography. Advantages of interstitial MRL include massively reduced doses of contrast media, more discriminatory accumulation in regional lymph nodes, and no harmful side effects. However, it is still unknown whether this approach allows differentiation between normal and tumor-bearing lymph

nodes or otherwise. Beyond the commercially available extracellular paramagnetic agents, other gadolin ium-based agents are now undergoing clinical testing.

2.7.2 MR lymphographic Imaging

It is well documented that MRL provides useful anatomical and physiological data, thus enabling accurate diagnosis of the disease. It is reported that the sensitively and specificity of the procedure is 90% and 94 %, respectively (Mitsumori et al., 2016).

Many authors reported the advantages of contrast studies, and others attempt to acquire images without contrast medium. MRL consists of two sequences. The first is a 3D heavily T2-weighted sequence to depict the severity and extent of the lymphedema. The second is a fat-suppressed 3D spoiled gradient-echo sequence performed after the intra-cutaneous injection of an extracellular gadolinium-based MR contrast agent (Mitsumori et al., 2016). In addition to that, the authors reported that as venous enhancement almost always occurs, one of the interpretative challenges is differentiating enhancing lymphatic channels from superficial veins.

Noncontrast MRL has substantial benefits as compared with other imaging techniques. In this context, Arrive et al. (2016), and Derhy et al. (2013) reported that Noncontrast MRL could be performed using heavily T2-weighted fast spin-

echo sequences (to demonstrate the location of edema) with long T2 relaxation time. Derhy et al. (2013) stated that 3D MRL demonstrates that retroperitoneal lymphatic aneurysmal dilatation. The authors reported that this technique was useful in diagnosing any clinical condition. In another recent study, Arrivé et al. (2017) used non-contrast MRL for the evaluation of lymph node for the secondary upper limb lymphedema. The authors used a free-breathing three-dimensional fast spin-echo sequence to evaluate the results of axillary lymph node transplantation with non-contrast MRL in 17 patients with secondary upper limb lymphedema. The study recommended that Noncontrast magnetic resonance lymphography might be used as a scientific technique to analyse the results of lymph nodes before and after the surgery. MR lymphography, with very heavily T2-weighted MR images, provides an excellent analysis of both lymphatics vessels and lymph nodes without need of any contrast media. Kim et al. (2016) assessed the thoracic duct using coronal and axial images of heavily T2-weighted sequences without contrast medium. Non-enhanced MR lymphangiography is a safe and practical technique for imaging the central lymphatic system and can contribute to differential diagnosis and appropriate preoperative evaluation of pathologic lymphatic problems. The main limitations to non-contrast T2 imaging are that it does not provide information about lymphatic flow, and the lack of a contrast medium makes it difficult to visualize

small lymphatic ducts. Consequently, its use in diagnostic and interventional lymphangiography is limited (Dori, 2016).

Recently, Cellina et. al., 2019 reviewed a non-contrast magnetic resonance lymphangiography as an emerging technique for the study of lymphedema. The authors concluded that non-contrast magnetic resonance lymphangiography, a relatively new technique for the diagnosis, assessment, and management of lymphedema.

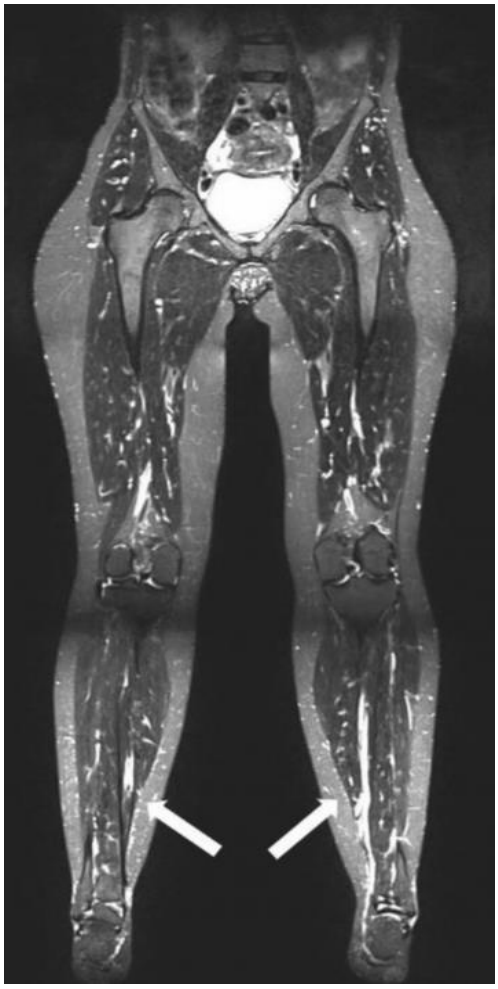

Figure 2.5: non contrast lower limb MRL for female patients (36 years old). The arrows showed collection of epifascial fluid (Cellina et al., 2020).

2.7.3 Non contrast MRL technique

2.7.3.1 Patient preparation and positioning

MRL without contrast can be performed using MRI system with magnet strength 1.5 or 3.0 T. Before positioning, it is important to explain in detail the diagnostic procedure and the need to maintain the position throughout the duration of the examination. According to the patient's size, the acquisition is usually performed in 3 or 4 steps to cover all the anatomical stations for both lower and upper extremities. The acquisition techniques described in the literature have provided for the acquisition of the entire limb in secondary lymphedema as well, to accurately define the extent and severity of the disorder and to perform an optimal post treatment follow-up (Figure 2.6) .

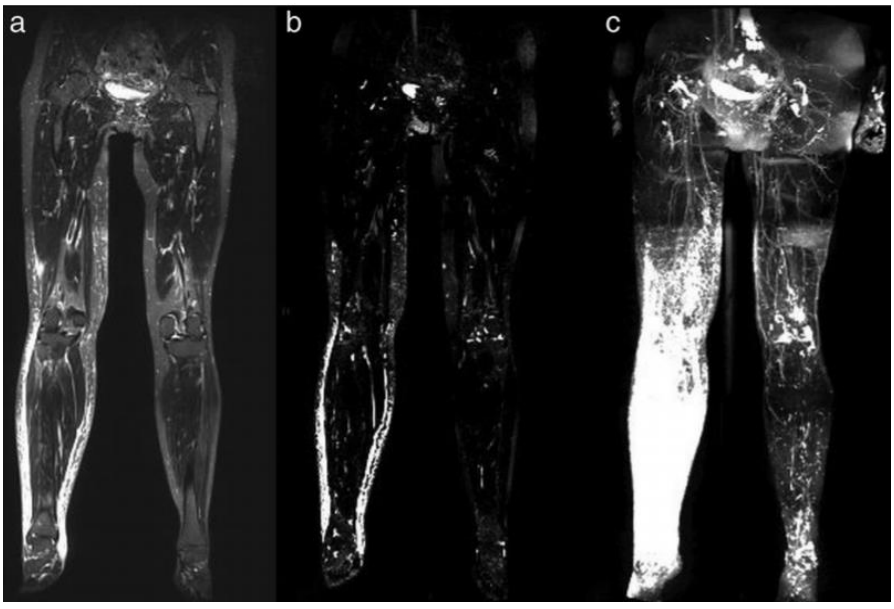

Figure 2.6. Non contrast MRI for female patient suffering from secondary lymphedema using (a) Short tau inversion recovery (STIR) sequence ,(b) T2 lymphographic sequence and (c) T2 lymphographic sequence with maximum intensity projection (MIP) reconstruction (Cellina et al., 2020) .

2.7.3.2 Acquisition protocol

Non contrast MRL technique is still evolving but the principle of this examination is based on heavily T2-weighted sequences, resulting in a signal loss in tissue background, by highlighting the static fluids in lymphatic vessels with a very long TR/TE, similar to that used in cholangiopancreatography or in MR urography. Acquisition parameters of non-contrast T2 MR Lymphography sequences are explained by various authors. Arrivé et al. et al. 2017, applied at the end of the echo train a restore pulse to flip the transverse magnetization to the longitudinal direction to reduce the acquisition time. Other sequences can be associated in the examination: axial HASTE without fat suppression (TR: 1200 ms, TE: 114 ms, matrix: 176×256, flip angle: 180°, slice thickness: 6 mm) or Iterative Decomposition of water and fat with Echo asymmetry and Least-squares estimation (IDEAL; acquisition plane: axial, TR: 4233 ms, TE: 76 ms, slice thickness: 6 mm, matrix: 320×192, FOV: 380×380), this sequence is based on fat/water separation technique, provides contrasts of water and fat, in phase and out of phase and is used for the analysis of lymphedema characteristics (Arrivé et al., 2017; Liu et al., 2005; Arrive et al.,2007).

In general Noncontrast MRL procedure with very heavily T2- weighted fast spin echo sequences is a useful non-invasive technique without the need of contrast medium injection to obtain a unique evaluation of the lymphatic system;

• To prove the lymphatic origin of a cystic formation, it is essential to demonstrate the communication with retroperitoneal lymphatic vessels

• 3D MR lymphography demonstrates that retroperitoneal lymphatic aneurysmal dilatation exhibits a continuous spectrum of change from normal variants to lymphatic aneurysmal dilatation and so-called cystic lymphangioma.

2.8 SPECT-CT/lymphography

Lymphoscintigraphy or hybrid imaging (SPECT/CT) is a specific, simple and reliable technique that offers useful information of lymphatic function, allowing the examiner to detect lymphatic flow obstructions, dilated vessels, collateral lymphatic flow and the presence, malfunction or absence of lymph nodes. Dermal activity uptake is a fundamental finding related to lymphedema (Witte et al., 2000). However, conventional lymphoscintigraphy has limitations related to its two-dimensional view, which does not allow a detailed spatial localization of tracer accumulation. Also, it cannot interpret secondary changes in connective-tissue such as fibrosis, nor can it accurately distinguish between dermal backflow and deeper lymph vessel accumulation (Maegawa et al., 2010) SPECT-CT is currently used with lymphoscintigraphy for sentinel node detection in breast cancer. In lymphedema, combined SPECT-CT/lymphography systems

provide integrated functional and morphological information, allowing a better localization in depth of vessels and lymph nodes, an accurate distinction between lymph vessels and veins and a correct interpretation of dermal backflow (Iimura et al., 2015). Combined CT-imaging has allowed a better comprehension of the physiopathology of lymphedema and many studies have proposed taking SECT-CT imaging beyond diagnosis and reported its value in microsurgical treatment as well. The incorporation of SPECT-CT in lymphedema staging might prove useful to predict treatment efficacy (Maegawa et al., 2010).

Lymphoscintigraphy and SPECT-CT imaging is used before surgery, for diagnosis, evaluation and treatment planning and one year after the procedure to evaluate the results. Studying all pre and postsurgical images obtained to the date, we have been able, as well as to classify the disease and decide the optimal treatment, to relate clinical outcomes to anatomic and functional images. For patients who present with limb lymphedema secondary to surgical lymphadenectomy clinically classified as stages III or IV and with SPECT-lymphography imaging that suggests absence of functioning lymph nodes associated to dermal backflow patterns, we propose microsurgical lymph node transfer.

2.9 CT lymphography

Computed tomography (CT) and magnetic resonance imaging are noninvasive techniques for diagnosing lymphangiomatosis; these imaging modalities identify fluid-filled masses in multiple organs. CTL technique with commercially available iodine medium has been adopted to preoperative evaluation of metastatic cancer to detect Sentinel lymph node before surgical operation. CTL provide visualized the correct number and position of SLNs, afferent and efferent lymphatic vessels connected to SLNs in 3D anatomy.

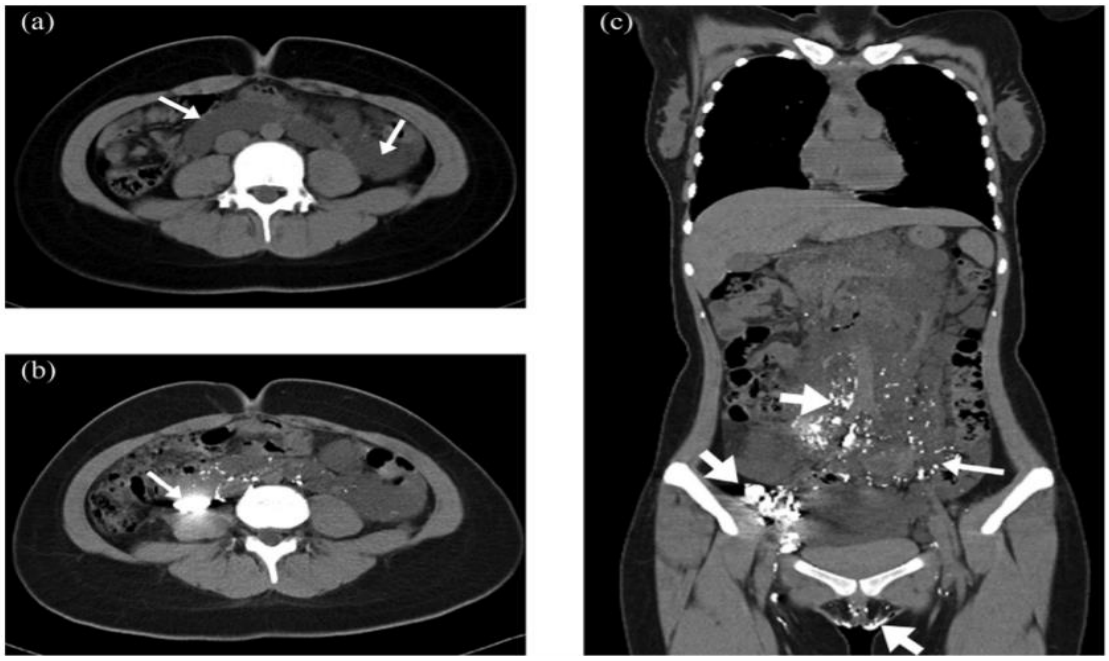

Figure 2.8 A routine admission nonenhanced axial CT scan showing multiple cystic lesions located in the mesentery and retroperitoneum (small arrows). (b) Axial CTL in the same plane as (a) showing contrast medium accumulation inside the cystic lesion on the right side of the retroperitoneum (small arrow). (c) Coronal CTL showing abnormal contrast medium distribution in the mesentery, retroperitoneum, and pelvis (large arrows). Finally, contrast medium was distributed on the contralateral side of the injected lower limb, indicating lymphatic reflux (small arrow).

CHAPTER THREE

MATERIALS AND METHODS

3. Materials and Methods

3.1 MR non contrast lymphography

3.1.1 Patient's populations

This study was conducted at IRCCS Policlinico San Matteo (PV), Pavia, Italy. A total of 17 patients were investigated for lymphedema evaluation during two years from October 2017 to October 2019. Inclusion criteria is pre and post-surgical operation while MRI contrast medium is a contra indication (Figure 3.1). Exclusion criteria include the use of contrast medium and age below 18 years. An informed consent was attained from all examined patients prior the procedure. The routine patient preparation include suspension of lymphatic drainage for two days and instructed to wear elastic stockings for one day. Patient communication is very crucial in order to maintain patient in the same position during the procedure. Patient is placed in the supine position, feet first, with both legs on a ramp pillow so that the lower extremity is parallel to the main magnetic field and near the most homogeneous area of B0.

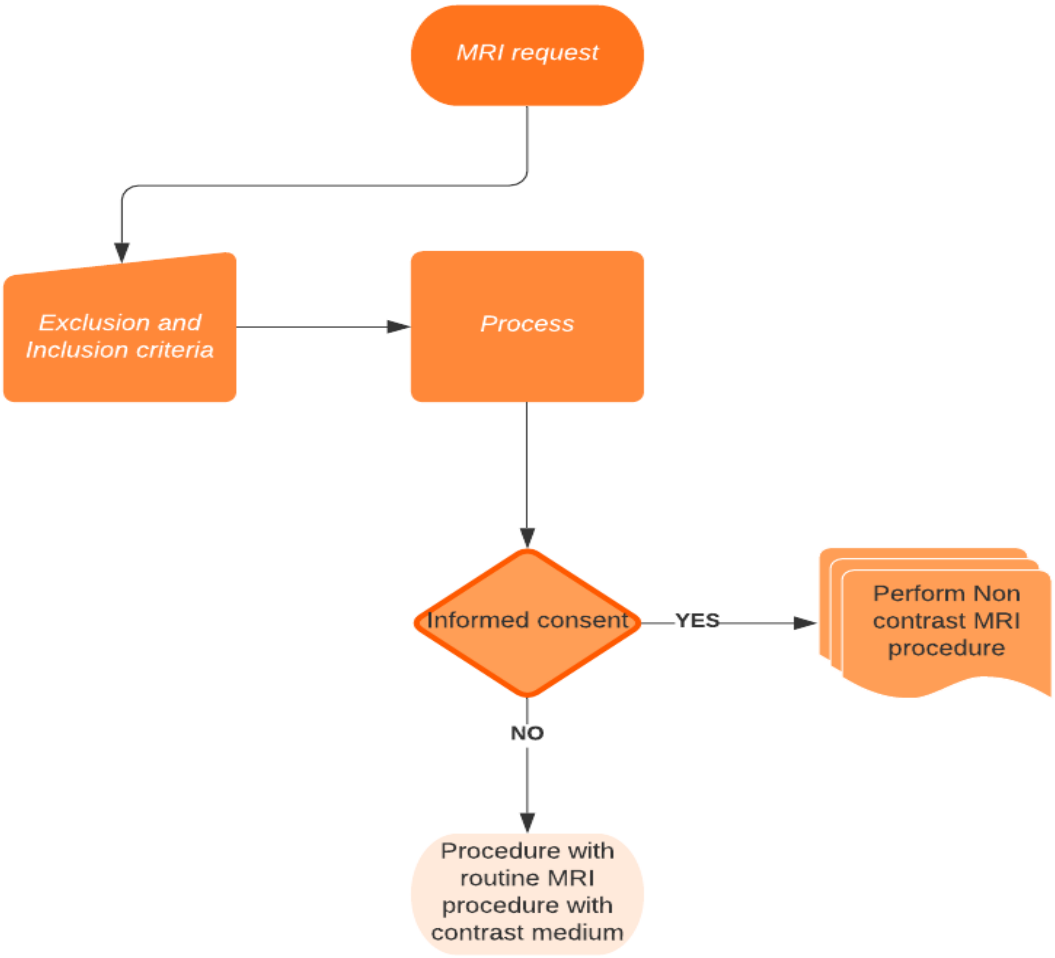

Figure 3.1: The flow chart shows the Noncontrast MRI procedure

3.1.2 Imaging equipment's

All procedures were performed using two MRI machines: Siemens Magnetom Aera 1.5T (Siemens Healthcare, Germany) (Figure 3.3). The machine with bore 60-cm bore delivers a complete range of clinical applications for whole body regions. The second machine is Philips MRI (ingenia) (Figure 3.3). The power

magnet of the machine enabled reduction in image acquisition time up to 50%. Both machines were subjected regularly to routine quality control test by a qualified medical physicist to ensure consistency and quality of the images.

Figure 3.2: Siemens Magnetom Aera 1.5T

Figure 3.3. Philips MRI (ingenia)

3.1.3 Imaging Protocol

The imaging protocol is composed of the standard sequences, according to Lymph Team protocol IRCCS Policlinico San Matteo (PV), using two MRI Scanners: Siemens Magnetom Aera 1.5T and Philips ingenia 1.5 Tesla. The sequences adopted for Siemens Magnetom Aera 1.5 T were consisted of 3D T2-weighed TSE with SPIR fat suppression. The sequences adopted were DT2-weighed HASTE with SPIR fat suppression. While the sequences used for Philips ingenia 1.5 consist of 3 acquisitions 3D T2 TSE oriented in axial, coronal and sagittal for each of the examined limbs. A single TSE sequence oriented in coronal plane is simply MRI cholangiography sequence modified by increasing the values of TR and TE. The parameters of the two type of sequences parameters are described in Table 1. The average time of the exam was about 30-45 min and a semi quantitative analysis of the exam was be used. For each procedure, at least six axial sections of each limb were investigated, and each of them was subdivided into four quadrants and evaluated according to specific score. A score of lymphedema severity (from 0 to 2 points) with a maximum of 48 points was used. The images were assessed by at least two radiologists with experience more than 15 years in addition to one resident. All the images were initially reported by one radiologist and revised by another one (double evaluation of the images).

Table 3.1. Patient image acquisition parameters according to acquisition type for Philips MRI (ingenia)

Parameter	2D	3D
Patient position:	Feet first	Feet first
Slice Thickness (mm)	5	1.8
Repetition time (ms)	1000	4000
Echo time(ms)	100	890
Number of averages	1	2
Spacing between slices (mm)	6	0.9
Echo train length	123	100
Acquisition matrix	320x280	500x450
Flip angle	90	90

3.2 CT Dosimetry in Lymphography

3.2.1 Patients populations

Effective dose for 28 patients undergone CT examinations for lymphedema as a clinical indication. All procedures were performed a tertiary hospital equipped with two CT modalities CT 128, 16 detectors from Siemens (Siemens Healthcare,

Germany). The two CT machines were calibrated to assure the accuracy of dose measurements. An accuracy of measured dose up to ±5% were obtained. The patient doses were estimated using measurements of CT dose indexes (CTDI), exposure-related parameters, and the ImPACT spreadsheet based on NRPB conversion factors (ICRP, 2007; Jones & Shrimpton, 2014; ImPACT, 2011). Data were collected using a sheet for all patients in order to maintain the consistency of the information displayed during CT examinations. All CT machines are equipped with a CT dosimetry unit. A data collection sheet was designed to evaluate the patient doses and the radiation related factors. The collected data include, sex, age, tube potential, tube current–time product settings, pitch, slice thickness and total slice number. Moreover, all the scanning parameters were recorded as well as the CT Dose Index volume (in millisievert) and dose-length product (in millisievert-centimeters).

3.2.2 CT dose measurements:

Radiation dose indicators volume CT dose index (CTDIvol (mGy)) and dose-scan length product (DLP (mGy.cm)). Tissue and organ equivalent dose conversion coefficient was obtained from the national protection board (NRPB), now health protection agency (HPA), datasets in the UK based on the Monte Carlo Simulations (Jones & Shrimpton, 2014). The CTDOSE dose analysis and estimation software developed by the ImPACT scan group was used to

extrapolate the effective and organ doses (Jones & Shrimpton, 2014, ImPACT, 2011). CT scan acquisition and exposure factors such as peak tube potential (kVp), tube current (mA), exposure time (second), pitch, slice thickness (mm), gender, and scan acquisition parameters were used to calculate the dose values.

3.2.3 CT lymphographic technique

CT lymphographic imaging was carried out for 28 patients using two CT modalities (128 and 16 Detectors). Ethics and research committee approved this retrospective study. Prior to image acquisition, patients were positioned in the supine with head first position. For the two modalities constant tube potential fixed at 120 kVp, different tube current and scan length was used for all patients (Table 3.2). The technique consisted of contrast and non-contrast CT image acquisition. Contrast medium injected at the area of the interest after local anaesthesia. Image acquisition was performed at certain time interval up to 10 min after the administration of the contrast media (Table 3.2).

Table 3.2. Patient exposure parameters during CTL (chest) procedures

CT Detector	Age (year)	Exposure setting (mAs)	Scan length (cm)
CT 128	36.0±10.0 (18.0-75.0)	190±60 (100.0-280.0)	53±77 (38.0-77.0)
CT 16	40.0±7 (30.0-64)	340±30 (210.0-255.0)	47.0±50.0 (42.0.0-55.0)

3.3. SPECT/CT Lymphography

3.3.1. SPECT/CT Imaging protocol

Patient preparation was based on individual patient's condition, but in general, no nutritional or medical treatment constraints were instituted for the procedure. The patients were instructed to be well hydrated before the SPECT/CT examination. Contrast was manually administered ^{99m}Tc sulfur colloid with an activity range of 18.5 MBq (0.2 mCi) to 40 MBq (1.1 mCi). In adult patients, ^{99m}Tc sulfur colloid, Tc- 99m human serum albumin (HSA), or Tc-99m nano-colloid albumin was injected into the skin for determination of lymph node drainage in breast cancer and malignant melanoma patients.

The imaging machine used was SPECT/CT [GE Hualun Medical Systems (Discovery NM/CT 670Pro)] which was equipped with Elite NXT detector technology comprising many features such as ultrashort photomultiplier tubes (PMTs) and a very thin, sensitive layer which enables high energy resolution and a high-count rate. The CT system consists of 16 slice CT (Bright-Speed Elite). The machine could also acquire high-quality SPECT/CT images without affecting the image quality.

Thirty patients have undergone lymphoscintigraphy for different clinical indications, as illustrated in Table 3.3. Lymphoscintigraphy helps to evaluate the body's lymphatic system for diseases using small amounts of radioactive materials called radiotracers that are typically injected into the bloodstream, inhaled, swallowed, or in the case of lymphoscintigraphy, injected into the skin. The radiopharmaceutical material is injected intradermally on the patient's right and left lower extremities in the 1st and 2nd web space of each foot. The surgical procedures are undertaken immediately after the procedure. The radiotracer travels through the area being examined and gives off energy in the form of gamma rays, which are detected by a special camera and a computer to create images of the inside of the body. Because it can pinpoint molecular activity within the body, lymphoscintigraphy offers the potential to identify lymphatic disease in its earliest stages.

Table 3.3. clinical indications of lymphoscintigraphy procedures

No	Clinical indications	No	Percentage
1	bilateral lower limb swelling	20	66.7
2	upper limbs after surgery	3	10
3	Sentinel lymph node mapping for Melanoma	4	13.3
4	Cancer (Sarcoma, hemangioma)	3	10
Total		30	100

3.3.2. SPECT/CT Image acquisition

Anterior and posterior static images of the lower limbs were obtained immediately for a one-hour dynamic image, and spot images were acquired two and four hours later. SPECT/CT of the pelvis and the lower limbs, including both knees, were also performed. Dynamic images of the feet were acquired for 30mins, followed by half body sweep images from the upper abdomen to the feet at one, two, and fourty-three hours. Images of the SPECT-CT of the pelvis were processed using the cinematic display of images viewed by the physician. No instructions were needed after the procedure.

3.3.3. SPECT/CT Patient Dosimetry

In the dosimetry tables, included here, the local radiation dose has been ignored, and the effective dose has been calculated under the assumption that fifth of the administered activity (20%) absorbed consistently (Kaplan et al., 1985). The reason for ignoring the local radiation dose is that deterministic effects (e.g., local skin necrosis) are not a concern for Tc^{-99m}–labeled radiopharmaceuticals. All patients who have undergone lymphoscintigraphy or SPECT/CT procedures for lymphedema were included in the study. Ethics and research committee at King Fahad Medical City approved the study. All data were collected retrospectively from the Picture Archive and Communication System (PACS) and patients record. The data collected were image acquisition protocol and patients' and staff's safety. Patient's data included age, body mass index (BMI(kg/m^2)), duration of lymphedema, location of disease, gender, and clinical indications. The effective doses (E) were estimated using the OLINDA software (Vanderbilt University**,** Nashville, USA), while the effective dose from CT was estimated using the ImPACT software (Saint George Hospital, London, UK).

CHAPTER FOUR

RESULTS AND DISCUSSION

4. Results and Discussion

4.1. MRL non contrast procedures

A total of 17 patients were enrolled in this study. All patients referred to the department for justified clinical conditions. No volunteer was included in this study. The number of patients were determined according to patients flow rate. All patients with pre and post non contrast or post-surgery were included in this study. Exclusion criteria include the use of contrast medium. Out of the 17 patient's populations, 4 (23.5%) patients were males while 13 (76.5%) patients were females. The mean age and range of patients group is 53.5±13 (26.0-76.0) as shown in Table 4.1. All patients with normal weight range with body mass index (BMI(kg/m^2)) range from 18.4 to 25.9. Out of the 17 patients, 4 (23.5%) patients had a primary lymphedema while 13 (76.5%) of the sample has a secondary lymphedema resulted from cancer treatment using radiation therapy or surgical intervention. 60% of the patients have underdone the procedures pre and post-surgical intervention.

Table 4.1. patients demographic data

Parameter	Mean±sd	Min	Max
Age (year)	53.5±13	26.0	76.0
Weight (kg)	61.1±11	50.0	77.0
Height (cm)	168.0±8	152	178
BMI (kg/m^2)	21.5±3.2	18.4	25.9

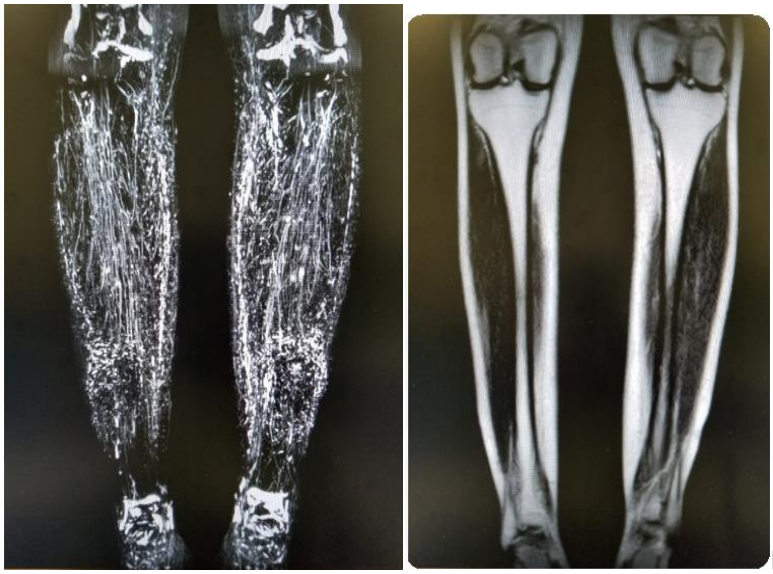

A B

Figures 4.1: A, B Non-contrast MRI for the leg of a 37 years old female patient suffering from secondary lymphedema due to radiation therapy (Left leg edema in 2012. She underwent lymph node transplantation in 2014, and at examination time, she has right leg edema.

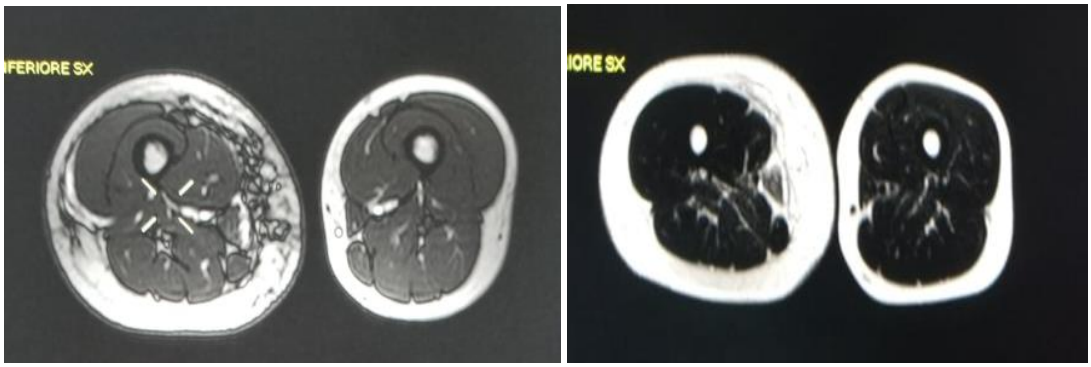

A B

Figure 4.2. A.B: non contrast MRI for 34 year old female patients suffering from lymphedema (left arm).

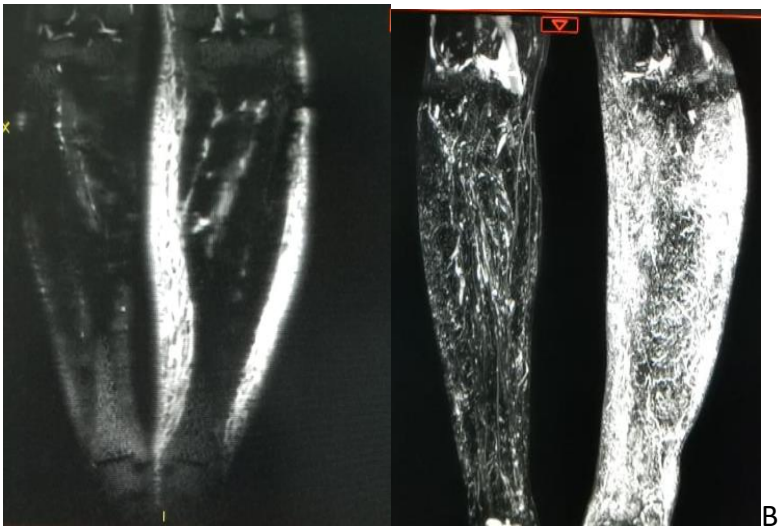

Figure 4.3: A,B Non contrast MRL for 65 years old female patients suffering from secondary lymphedema pre and post-surgery. She underwent auto transplantation in 2015.

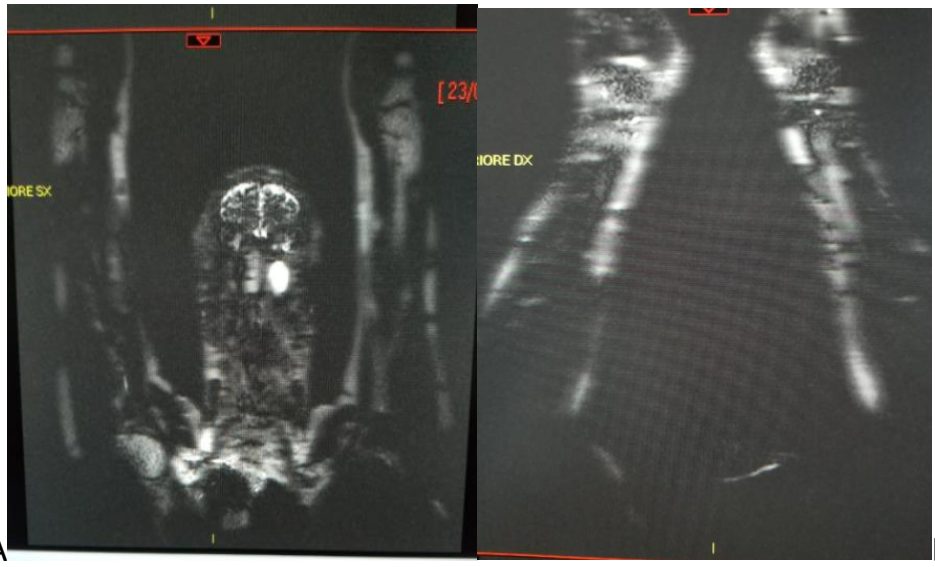

Figure 4.4: A,B Idiopathic edema of the right arm for male patients 44 years old, due to primary lymphedema. The patient underwent lymph node transplantation in 2014. Significant lymphedema (right arm). Pre and post transplantation.

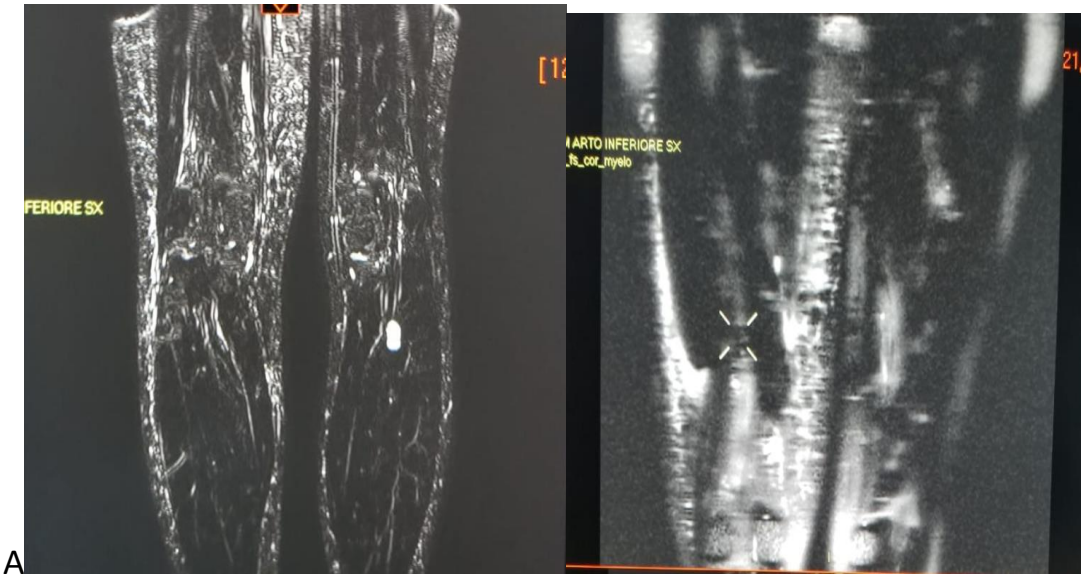

A B

Figure 4.5: A, B: Non contrast MRI for 34 years old female pre-and post non contrast MRI

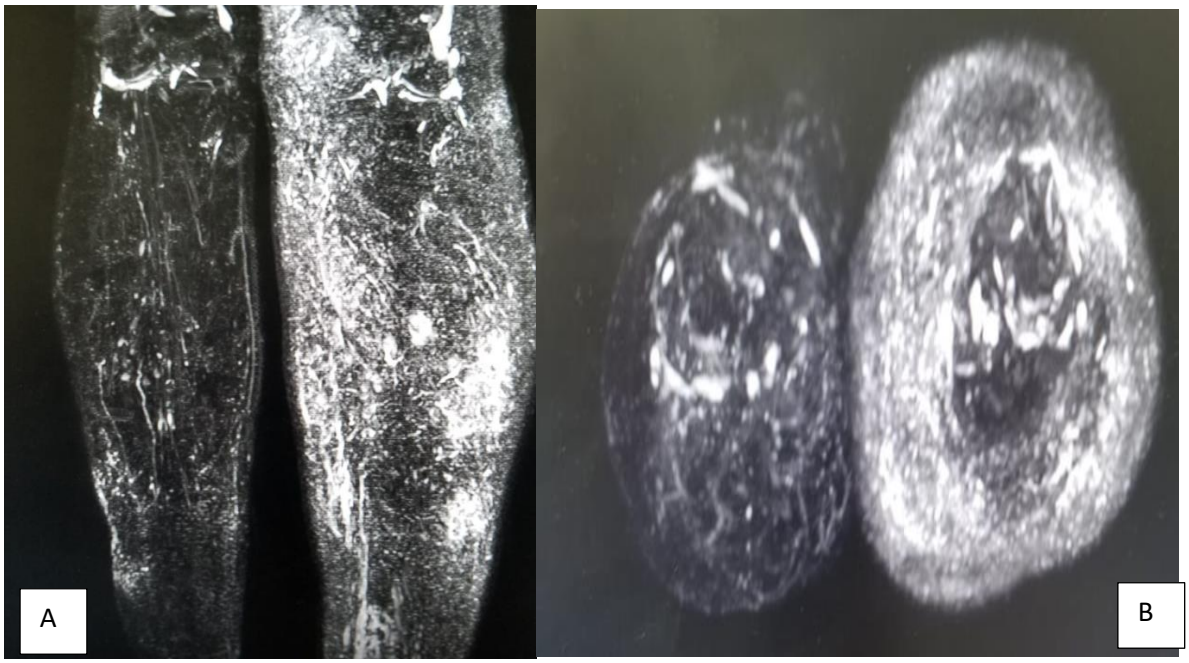

Figures 4.6: A &B : Non contrast lower limb MRI for 54 years old female patient suffering from secondary lymphedema (moderate lymphedema). Pre and post transplantation non contrast MRI.

Non contrast MR-Lymphographic technique has a capability in providing high-resolution images of the lymphatic system with very good anatomical findings. Thus, this promising technique can be used with patients with contra indication to the contrast medium or patients with low Glomerular Filtration Rate (GFR). Non contrast MRI technique has an excellent potential in providing accurate and reliable diagnosis and planning of microsurgical intervention. Figure 4.2 showed arm images for non-contrast MRI procedures. Figure 4.3 A, B Non contrast MRL for a 65 years old female patient suffering from secondary lymphedema pre and post-surgery. 35% of all cases were undergone post-surgery non contrast MRL while 65% of the cases undergone pre and post MRL. All the 17 cases, who undergone MRI without contrast for lymphedema had diagnosable images and provided acceptable findings, thus no image was rejected or considered poor. The development of MRI technology using string magnetic field with sensitive coils and advanced image processing software, enabled operators to reduce the scan time and increase image quality. Ass illustrated from the current study results, the vast majority of clinical indications is secondary lymphedema due to acquired cause (radiotherapy or surgery). Primary lymphedema incidence occurs always for patients below the age 35 years old. However, only 4 patients undergone the procedure suffering from primary lymphedema. The clinical manifestations of primary lymphedema occur in patients from birth to over 25

years of age. Arrivé et al., (2017) reported that non-contrast MRL is useful imaging procedure for the diagnosis of the extremities, patient follow up and severity assessment, classification, and follow-up. The advantages of the contrast medium studies include accurate delineation of the anatomical details of the lymphatic and vascular systems (Hsu & Itkin., 2016). In this research, non-contrast MRI study was used to evaluate patients' pre and post microsurgery or physical therapy (Campisi et al., 2006). In agreement with previous studies, and after rigorous assessment of patients using pre and post non contrast imaging, patients were benefited from microsurgery, particularly the patients who were at the early stage of the disease by decreasing the swelling and quick recovery (Campisi et al., 2006). NCMRL is used for evaluation of lymphedema in literature (Almujally & Calliada, 2020). However, this study provided unique assessment of patient's pre and post micro surgery. The image acquisition sequences consisted of 3D T2- weighed TSE with SPIR fat suppression. The sequences adopted were D T2- weighed HASTE with SPIR fat suppression. While, the sequences used for Philips MRI (ingenia) consisted of 3 acquisitions 3D T2 TSE oriented in axial, coronal and sagittal for each of the examined limbs. A single TSE sequence oriented in coronal plane (it is simply MRI cholangiography sequence modified by increasing the values of TR and TE). Comparable sequences were reported by Arrive at al., (2019) which included 3D high spatial

resolution, fast-recovery, fast spin-echo (FRFSE). The current imaging sequences enabled acquisition of high image quality (high signal-to-noise ratio (SNR), which means to obtain diagnosable image quality while overcoming the contrast medium disadvantages.

On the other hand, Lymphoscintigraphy is an effective tool for the assessment of limb lymphedema, it is the generalized imaging technique used for its diagnosis and classification and also for pre-surgical planning (Yamamoto et al., 2011; Szuba et al., 2003).

One of the promising treatments is microsurgical intervention. Lymph venous shunt is the prime therapy of lymphedema in addition to the lymph nodes transplantation (Garza et al., 2017). Critical Investigation of lymphedema is crucial to provide differential diagnosis, to confirm the diagnosis, to assess the severity and extension of lymphedema and to allow an adequate treatment planning. All imaging techniques have advantages and disadvantages for assessment of the lymphedema. Lymphoscintigraphy is performed by injecting intradermal Technetium 99m sulfur colloid; the progression and the distribution of the radio-labelled particles is evaluated by a gamma camera, but subdermal lymphatics cannot be assessed (Yoshida et al., 2016).

Non-contrast MRL is an improved technique and showed the significant diagnostic values with minimal contraindications and side effects. This

technique allows clear visualisation of lymphatic system vessels, thereby enabling the accurate diagnosis with high accuracy.

Cellina et al.,(2019) and Arrive et al.,(2018) report that non contrast MRL enables the radiologists to obtaining differential diagnosis between lymphedema and lipoedema and between lymphedema and phlebedema of the of the lower limb. This is due to the fact that phlebedema is characterized by an involvement of the subfascial muscular compartment appearing as dimensional increase, muscle edema or fatty degeneration (Case et. al., 1992). Cellina et al., (2019) reported that lymphedema was a condition limited to the subcutaneous fat tissue as illustrated in Figure 4.7

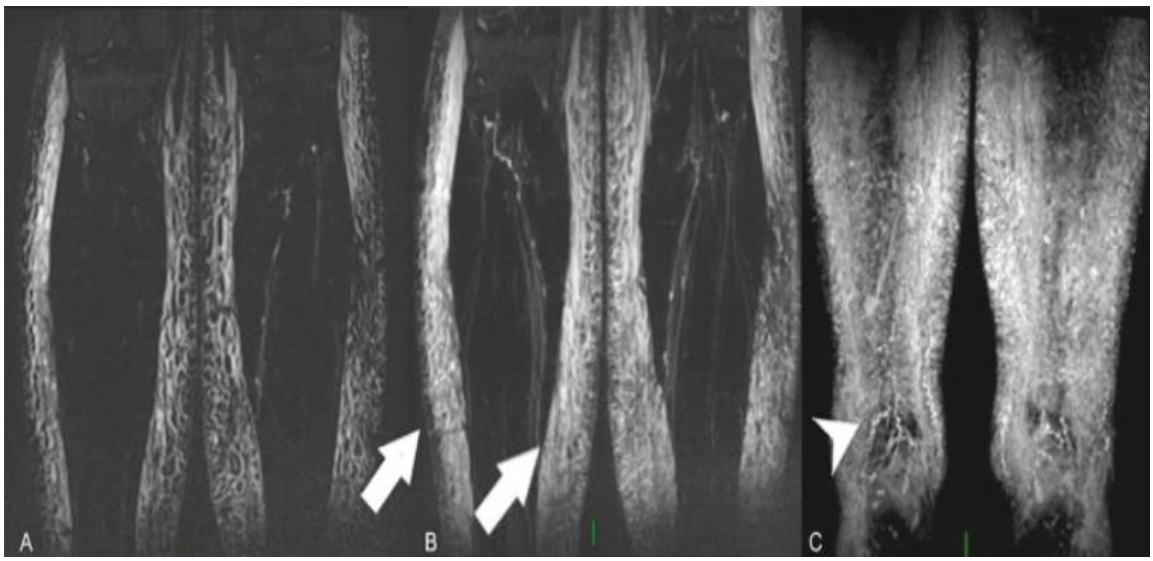

Figure 4.7 Congenital lower limb lymphedema (30 years old male patient (Cellina et al., 2019).

This study and the previous studies (Cellina et al., 2019; Arrive et al., 2018) form a conclusion that non contrast MRL is a useful imaging technique for the analysis of lymphedema. It is also used for microsurgery and effective tool for differential diagnosis.

CT is useful imaging technique for certain procedures. Hadjis et al., (1984) reported that CT findings in patients with primary lymphedema by comparing them with patients with swollen legs, secondary to chronic venous disease or lipedema, was important and the honeycomb pattern was not seen in any of the latter patients. Moreover, other studies reporting the CT appearance of lesions of the lower limb, including tumors, abscess, and hemorrhage, have failed to demonstrate a specific pattern. If this pattern specificity were to be confirmed by CT findings in a larger series, it could form the basis for noninvasive diagnosis of primary lymphedema.

The main limitation of NCMRL procedure is the fact that lymphedema is common in obese patients, therefore obese patients grade three cannot be examined in close magnet bore due to their weight and non-contrast MRI is usually performed on 1.5 T magnet or above. Therefore, open magnet technique cannot be used which is one of the limitations of this technique.

Table 4.1. Advantages and drawbacks of various imaging modalities

Imaging modality	Drawbacks	Advantages
Lymphangiography	Fever, Infection and lymph vessels inflammation, contrast medium remain for up to 2 years in lymph nodes	Demonstrate disorders of the internal tissues of lymph nodes
lymphoscintigraphy	Low image resolution, prolonged procedure time cost, radiation dose	lymphatic function
Indo cyanine green-lymphography (ICG-L)	cannot detect deep lymphatic vessels ($\leq$ 2 cm)	insignificantly invasive, simple, Real-time imaging and sensitive.
Computed Tomography	Limited contrast resolution Radiation risk	Cheap, low cost
Magnetic resonance lymphangiography (MRL)	Contrast medium Can not differentiate benign and cancer tumors	Excellent anatomy high spatial resolution No radiation exposure 3D image physiological information high soft tissue contrast
Non-contrast Magnetic Resonance Lymphangiography (NCMRL)	Suspension the lymphatic drainage for 48 h. Elastic stockings or bandages for 24 h.	No contract medium illustrate static fluid-filled lymphatic vessels, safe and feasible

NCMRL has some limitations. First of all, diagnostic experiences with this relatively new technique are few as as: more investigations with larger patient case series are still needed to validate the use of this examination; to accurately

determine the areas of application, it needs to improve the technique. It is well documented that dilated lymphatic is well demonstrated by NCMRL, however, NCMRL cannot illustrate normal or hypo-plastic lymphatic structures, as described by Liu et al., (2005). Furthermore, due to the absence of the gadolinium as a contrast medium, NCMRL does not provide physiological findings regarding the timing of the lymphatic drainage or the nodal uptake, unlike the contrast enhanced MRL (Cellina et al., 2019).

In addition to that, NCMRL has inadequate image spatial resolution as compared with the contrast enhancement MRL images. Thus, contrast enhancement procedure is the imaging technique of choice for assessment of distal lymphatic vessels, while non contrast MRL is the technique of choice for the assessment of proximal lymphatic vessels (Arrive et al., 2018).

Although so far not reported by the studies in the literature, we must also consider as a limitation the possibility of confounding influence of fat; therefore, according to our experience, the sequences without fat saturation are useful for an optimal evaluation of the extension of size increase of the involved limbs and to obtain reproducible measurements, especially is useful in the follow-up of treatment. On the other side, the heavily T2-weighted sequences are resulting signal loss in tissue background, with highlighting of static fluids, allow the visualization of epifascial fluid components and lymphatic vessel. The most

important advantage of this technique is the non-invasiveness and the non-need to administer contrast medium, this means great benefits for allergic patients and for paediatric patients, who can safely undergo this type of examination, and pose no risk related to gadolinium deposition. Moreover, the absence of contrast medium results in lower costs, when compared to CEMRL. Another advantage against CEMRL is the short acquisition time. In half an hour, patient positioning and imaging acquisition of the whole lower limbs can be performed, while for CEMRL a total average examination time of one hour and fifteen minutes for the lower limb is expected ((Arrive et al., 2018).

4.2. CTL dosimetry

Patient's doses during CT procedure including chest and lower or upper extremities is illustrated in Table 4.1 &4.2. The mean patient doses in term of $CTDI_{vol}$ (mGy) and DLP (mGy.cm) are 10.0 ±3 and 425±222 and 24±12 and 1118±812 for CT 128 and CT 16 slice, respectively. The results show that the patient dose from CT 16 slice is double the dose from 128 slice. A huge variation up to 100% exists between the two imaging modalities. This can be attributed to variation exposure parameters selection and imaging protocol. Patient effective dose also shows the same level of variation since the patient group are within the same age range and a considerable variation of mean organ doses

among hospitals was observed for similar CT examinations. In addition to that, patient's doses showed three time variation between the minimum and maximum values suggesting that imaging protocol should be standardised and be optimised. The mean scan length always and tube current time product (mAs) are in direct proportional relation with patient doses. Thus, precise adjustment of these factors will result in drastic reduction of patient dose without deteriorating the image quality. The mean effective dose (mSv) per procedure is 6.6±3 and 15.7±12 for CT 128 and CT 16 slices, in that order. The effective dose for CT lower extremities is lower as compared to CT abdomen and pelvis. This can be attributed to the fact that most of the human radiosensitive organs and tissues are located in the trunk region. The lower DLP to effective dose conversion factor was used as compared to CT chest and abdomen. The prospects of radiogenic risk due to ionising radiation exposure depend on irradiated organ doses, age at exposure, and patient tissue or organ weight. The patient radiogenic risk per CT examination is ranged from 35 to 70× 10^{-5} per procedure. The current practice showed that patients usually exposed to high dose exceeding 100 mSv in a year due to their diagnosis and treatment follow-up.

Table 4.2: Patient doses during CTL procedures

CT Modality	$CTDI_{vol}$ (mGy)	DLP (mGy.cm)	Effective dose (mSv)
CT 128	10.0±3 (5.0-14.0)	475±220 (166.0-950.0)	6.6±3 (2.3-13.3)
CT 16	24.0±12 (13.0-36.0)	1118±812 (545-1695.0)	15.7±12 (7.6-23.7)

Lymphedema patients undergo a series of imaging procedures including nuclear medicine procedures such as single photon emission computed tomography (SPECT) or positron emission tomography (PET) with sensitivity up to 96% (Hassanein et. al., 2017). In literature, to our knowledge, this is the first study provided radiation dose for lymphedema patients undergoing CT procedures. Various organs in the primary beam received high radiation dose. Breast, lung and heart received equivalent dose (mSv) 30, 32, 35 mSv per single procedure respectively. This high organ doses increase the risk of radiation induced cancer for these specific organs especially for the young patients. All

previous study reported the dose value for specific organs (chest, abdomen, brain or extremities) for different clinical indications. Thus, this study provided a new information regarding the radiation risk for lymphedema patients in comparison with previous studies (Sulieman et al., 2015; Tsalafoutas et. al., 2010; Lam et al., 2015) (Figure 4.4).

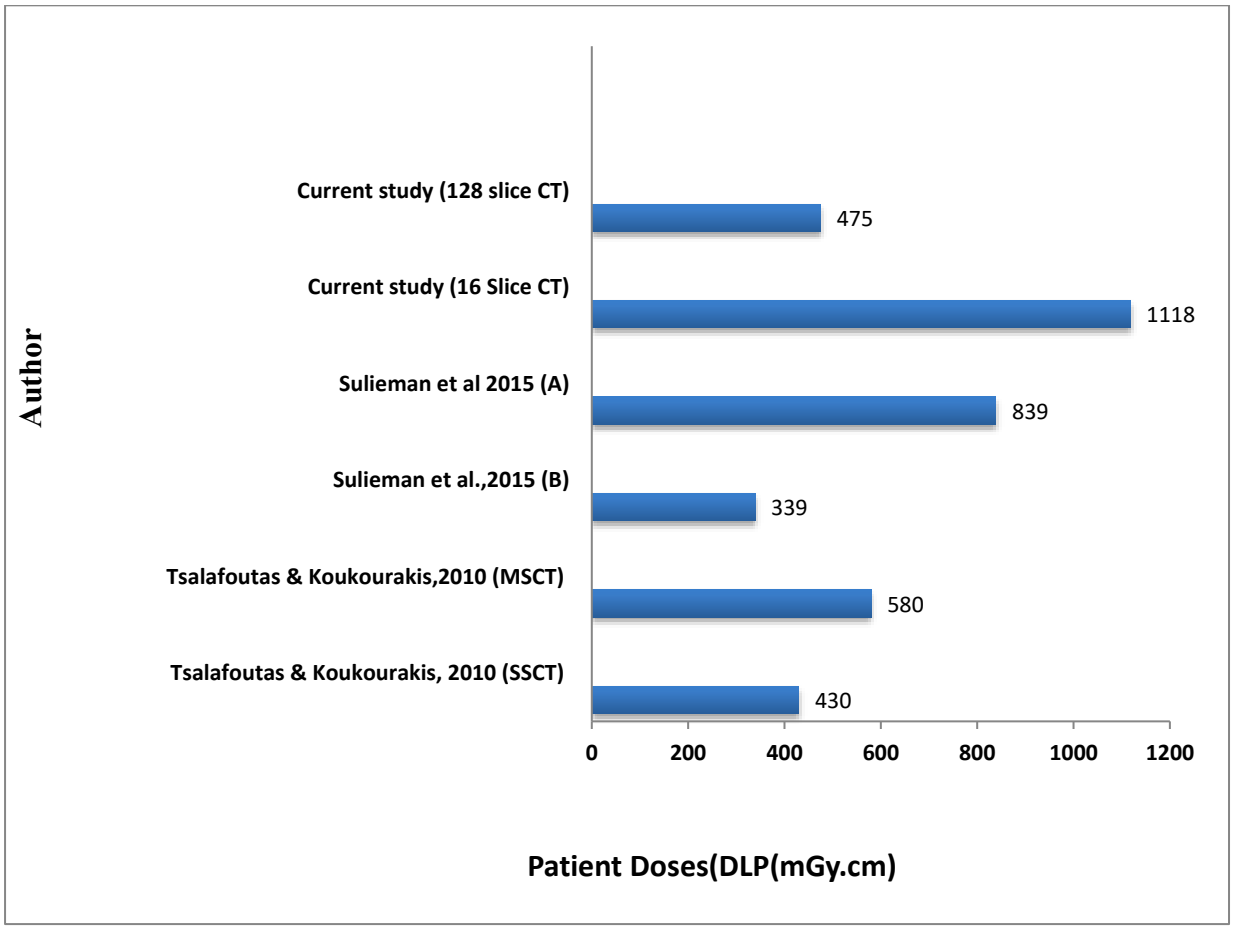

Figure 4.4: Comparison of patient dose during chest CT procedure. (MSCT: multi slice CT, SSCT, Single slice CT,A control group, B: optimization group).

The current study dose is higher as compared with conventional CT procedures because in this study additional image acquisition is required to provide further

details according to the clinical indication (Manssor et al., 2015; Sulieman et al., 2011). However, still dose can be optimised to assure that patients receive a minimum radiation dose.

4.3 SPECT CT dosimetry

Table 4.4 shows the administered radiopharmaceuticals for patients during lymphoscintigraphy by using a hybrid system (SPECT/CT) according to the King Fahad Medical City (KFMC) imaging protocol. The effective radiation doses during SPECT/CT lymphoscintigraphy depend on the exposure parameters for the CT machines and the amount of the administered activities.

Table 4.4. mean, standard deviation and range of patients demographic data and administered activity

Gender	No	Age (y)	Height (cm)	Weight (kg)	Activity (mCi)	Activity (MBq)	Effective dose (mSv)
F	19	45.05±16 (12-75)	154.79±6 (144-162)	92±25 (46-145)	0.56±0.2 (0.5-1.1)	21±6 (18.5- 40.7)	0.21±0.01 (0.19-0.41)
M	11	40±17 (12- 57)	168±19 (132-181)	(105±22 (61-121)	0.58±0.2 (0.51.0)	21.6±8 (18.5- 37)	0.22±0.01 (0.19-0.4)
Overall	30	44±16 (12-75)	158±11 (132-181)	(95±25) (46-145)	0.57±0.2 (0.5-1.1)	21±7 (18.5-40.7)	0.21±0.01 (0.19-0.41)

Of the thirty patients who were undergone SPECT/CT in this research, 63.3 % and 36.7 % were females and males, respectively. Table 4.5 presents patients' characteristics (age (y), and height (m)) and the administered activity per patient. The effective dose (mSv) per procedure ranged from 0.19 to 0.41 mSv, with an average dose value of 0.22 mSv (Suga et al., 2001; Ohtake et al., 1986). There was no variation between administered activity and patient's effective doses according to the gender. During CT examination as a part of the SPECT/CT procedure, patients received higher doses as compared with the effective doses they got from the administration of ^{99m}Tc sulfur colloid.

Table 4.5: CT exposure parameters and patients doses during SPECT/CT examination

Tube potential (kVp)	Tube current – time product (mAs)	rotation time (s)	slice thickness (mm)	pitch	CTDIvol (mGy)	DLP (mGy.cm)	Effective dose (mSv)
120	80	0.8	3.75	1.375	4.11	241.4±74 (178.8-324.1)	0.05±0.01 (0.04-0.1)

The average effective dose obtained from CT examination was 0.05; ranging from 0.04 to 0.1 mSv per procedure. The effective dose in CT was therefore lower than that of the SPECT procedure by a factor of 5. This was attributed to the low radio sensitivity of the lower limbs because no sensitive organs were

included in the primary beam. During SPECT/CT lymphoscintigraphy examinations, the radiation dose was low as compared with other SPECT/CT imaging procedures or even during separate SPECT or CT procedures. This low dose was due to the small amount of administered activity and low exposure parameters. From Table 3, the CT imaging protocol is based on fixed exposure parameters. The effective dose (mSv) conversion factor from DLP (mGy.cm) is comparable with the value reported by Saltybaeva et al., (2014) (0.0002 mSv/DLP (mGy.cm)). The overall patient radiation dose of SPECT/CT is the summation of the effective dose due to the radiopharmaceutical material injected (^{99m}Tc sulfur colloid) for SPECT image acquisition and the effective CT dose resulting from external radiation exposure. Therefore, careful radiation dose optimization during SPECT/CT procedures will reduce the patient doses to the lowest possible level without affecting the clinical findings (Ferrari et al., 2014).

For this reason, the radiopharmaceutical material used and its administered activity, as well as the image acquisition and processing modalities both in SPECT and in CT must be carefully evaluated. The use of SPECT/CT lymphoscintigraphy procedures in clinical practice is important due to its ability to demonstrate the lymphatic vessel drainage patterns. Therefore, with a low dose per procedure, the surgeon can use the imaging without any increase in radiation risk. The

current radiation risk from SPECT/CT is equivalent to 7 months of natural background radiation exposure. This places it under the category of low radiation risk for cancer, equivalent to 1 cancer case per 10^5 SPECT/CT lymphoscintigraphy procedures.

Buck et al., (2008) showed that the effective dose of SPECT/CT ranged from 0.19 to 0.41 mSv using low dose imaging protocol per procedure, which is higher than the current study. However, Roach et al. (2006) reported comparable values to our study, ranging from 1–2 mSv per SPECT/CT procedure. In addition, patients' effective doses (mSv) per SPECT/CT for chest, abdominopelvic, and head were reported to be 1.1, 1.3, and 0.2 mSv respectively (Sawyer et al., 2008).The CT dose during SPECT/CT is within the diagnostic reference level values range that was proposed by Avramova-Cholakova et al., (2015) (CTDIvol= 4 mGy, DLP (mGy.cm) =120 and ad mistered activity (MBq) = 74).

5. Conclusions

The current study shows that MRL is useful and reliable procedures for the diagnosis and follow up patients with lymphedema pre and post-surgery. The current imaging protocol enabled acquisition of diagnosable MRL images. The current imaging sequences enabled acquisition of high image quality (high signal-to-noise ratio (SNR), which means diagnosable image quality while overcoming the gadolinium disadvantages. Early Lymphedema stage diagnosis is a great challenge. Non contrast MRL is used to diagnose accurately the lymphatic system disorder and can be used for differential diagnosis or with patients with contraindications for gadolinium. The study reveals that non-contrast MRL imaging technique can increase the accuracy of lymphedema diagnosis, improves disease prognostication, and provides a more robust marker of treatment response. Patient radiation dose during CT and SPECT/CT lymphoscintigraphy is one of the drawbacks of these imaging procedures. Non contrast MRL is a promising methodology in the diagnosis of lymphatic system disorders with a reasonable accuracy.

Bibliography

Avramova-Cholakova, S., Dimcheva, M., Petrova, E., Garcheva, M., Dimitrova, M., Palashev, Y., & Vassileva, J. (2015). Patient doses from hybrid SPECT–CT procedures. Radiation Protection Dosimetry, 165(1-4), 424–429.

Arrivé L, Derhy S, El Mouhadi S, Monnier-Cholley L, Menu Y1, Becker C.(2016). Noncontrast Magnetic Resonance Lymphography. J Reconstr Microsurg. 32(1):80-6.

Arin K. Greene MD, MMSc, Sumner A. Slavin MD, in Plastic Surgery Secrets Plus (Second Edition), 2010.

Arrivé L, Monnier-Cholley L, Cazzagon N, Wendum D, Chambenois E, El Mouhadi S. (2019).Non-contrast MR lymphography of the lymphatic system of the liver. Eur Radiol. 29(11):5879-5888.

Arrivé L. , L. Azizi, M. Lewin, C. Hoeffel, L. Monnier-Cholley, C. Lacombe, et al. (2007). MR lymphography of abdominal and retroperitoneal lymphatic vessels. AJR Am J Roentgenol, 189 (5) , pp. 1051-1058.

Arrivé L. , S. Derhy, C. Dlimi, S. El Mouhadi, L.Monnier-Cholley, C. Becker. (2017). Noncontrast magnetic resonance lymphography for evaluation of lymph node transfer for secondary upper limb lymphedema. Plast Reconstr Surg, 140 (6) . 806-811.

Arrivé, L., Derhy, S., Dahan, B., El Mouhadi, S., Monnier-Cholley, L., Menu, Y. ,et al. (2018). Primary lower limb lymphoedema: classification with non-contrast MR lymphography.Eur Radiol, 28 (1), 291-300.

Aschen SZ, Farias-Eisner G, Cuzzone DA, Albano NJ, Ghanta S, Weitman ES, et al. (2015=4). Lymph node transplantation results in spontaneous lymphatic reconnection and restoration of lymphatic flow. Plast Reconstr Surg. 133(2):301–10.

Aspelund, A., Robciuc, M., Karaman, S., Makinen, T., Alitalo,K (2016). Lymphatic System in Cardiovascular Medicine. Circ Res. 2016;118:515-530 .

Brenner, D, Hall, E. (2007). Computed tomography - an increasing source of radiation exposure. N Engl J Med 2007; 357: 2277-2284.

Buck AK, Nekolla S, Ziegler S, Beer A, Krause BJ, Herrmann K, Scheidhauer K, Wester HJ, Rummeny EJ, Schwaiger M, Drzezga A (2008). SPECT/CT. J Nucl Med 49:1305–1319.

CarrascoV , CarretoA , Garcia-Tutor E , de la Fuente E , López A , Alonso-Burgos A et al. MR -Lymphography: Technique, indications and results. ECR 2015.

Cosmus and Parizh. (2011). Advances in Whole-Body MRI Magnets. IEEE Transactions on Applied Superconductivity 21, Issue 3, 2104 – 2109.

Case, T.C. , Witte, C.L. , Witte, M.H. , Unger, E.C. , Williams, W.H.(1992). Magnetic resonance imaging in human lymphedema: comparison with lymphangioscintigraphy.Magn Reson Imaging, 10 (4), 549-558

Cellina M, Martinenghi C, Panzeri M, et al. (2020). Noncontrast MR Lymphography in Secondary Lower Limb Lymphedema [published online ahead of print, 2020. J Magn Reson Imaging.10.1002/jmri.27328.

Damadian R, Goldsmith M., L. Minkoff (1977). NMR in cancer: XVI. Fonar image of the live human body‖, Physiological Chemistry. and Physics, Vol. 9, 97-100.

Davies F.J (2000). MRI Magnets, Applications of Superconductivity, NATO ASI Series, Vol . 365, Kluwer Academic Publishers, 385-414.

Derhy S, El Mouhadi S, Ruiz A, Azizi L, Menu Y, and Arrivé L. (2013) Non-contrast 3D MR lymphography of retroperitoneal lymphatic aneurysmal dilatation: a continuous spectrum of change from normal variants to cystic lymphangioma. Insights Imaging. 4(6): 753–758.

Dori Y. Novel Lymphatic imaging technique. Techniques in Vascular interventional radiology. 2016.

Franconeri, A., Ballati, F., Panzuto, F., Raciti, M. V., Smedile, A., Maggi, A., Calliada, F. (2020). A proposal for a semiquantitative scoring system for

lymphedema using Non-contrast Magnetic Resonance Lymphography (NMRL): Reproducibility among readers and correlation with clinical grading. Magnetic Resonance Imaging. doi:10.1016/j.mri.2020.02.004.

German Cancer Research Center webste, dkfz.com.

Gough, MH. (1964,). Lymphangiography in children. Arch. Dis. Childh., 39, 177.

Huang,J, GardenierJ, Hespe,G , García G et al. (2016). Lymph Node Transplantation Decreases Swelling and Restores Immune Responses in a Transgenic Model of Lymphedema. PLoS One. 11(12): e0168259.

ICRP, 2007. International Commission on Radiological Protection. 2007. The 2007 Recommendations of the International Commission on Radiological Protection. ICRP publication 103. Ann ICRP 2007, 37(2-4): 1-332.

IMAIOS, 2020. MRI instrumentation. Avaialable at https://www.imaios.com/en/e-Courses/e-MRI/MRI-instrumentation-and-MRI-safety/Radiofrequency-system. Accessed August,6,2020.

ImPACT, 2011. CTDosimetry (version 1.0.4). Available at: http://www.impactscan.org/ctdosimetry.htm. Accessed May 13, 2020.

Jiang, X., Tian, W., Nicolls, M., Rockson, S. (2019).The Lymphatic System in Obesity, Insulin Resistance, and Cardiovascular Diseases. Front. Physiol.,10(1402), 1, 1-10.

Jones, D, Shrimpton, P (2014). Normalised Organ Doses for X-Ray Computed Tomography Calculated Using Monte Carlo Techniques. National Radiological Protection Board. NRPB-SR250. Chilton.

Kaplan WD, Piez CW, Gelman RS, et al. (1985). Clinical comparison of two radiocolloids for internal mammary lymphoscintigraphy. J Nucl Med 1985;26:1382–1385.

Kim et al.(2016). Anatomic and Functional Evaluation of Central Lymphatics With Noninvasive Magnetic Resonance Lymphangiography. Medicine. 95(12):e3109,1-8.

Lam, D., Larson, D, Eisenberg, J, Forman, H, Lee, C. (2016). ommunicating Potential Radiation-Induced Cancer Risks From Medical Imaging Directly to Patients. Am J Roentgenol. 205(5):962-70.

Liu N. , C. Wang, M. Sun. (2005). Noncontrast three-dimensional magnetic resonance imaging vs lymphoscintigraphy in the evaluation of lymph circulation disorders: a comparative study. J Vasc Surg, 41 (1) . 69-75.

Lvovsky Y. and P. Jarvis (2005). Superconducting Systems for MRI – Present Solutions and New Trends‖, IEEE Trans. Appl. Supercond., Vol. 15, , 1317-1325.

Magnetic Resonance Imaging (MRI) Equipment. A Global Strategic Business Report‖, MCP-3342, Global Industry Analysis, Inc., 2008.

Marken K., John Hulm (2004). Memorial Session, Applied Superconductivity Conference, Jacksonville, FL, 2004, unpublished.

Mitsumori LM, McDonald ES, Neligan PC, Maki JH.(2016). Peripheral Magnetic Resonance Lymphangiography: Techniques and Applications. Tech Vasc Interv Radiol. 19(4):262-272.

Modica M., S. Angius, L. Bertora et al. (2007). Design, Construction and Tests of MgB2 Coils for the Development of Cryogen Free Magnet‖, IEEE Trans. Appl. Supercond., 17,. 2196-2199.

Morrow G.(2000). Progress in MRI Magnets, IEEE Trans. Appl. Supercond., Vol. 10. 744-751.

Nadolski GJ, Itkin M (2013). Thoracic duct embolization for nontraumatic chylous effusion: Experience in 34 patients. Chest 143:158-163.

Ohtani O, Ohtani Y (2012). Recent developments in morphology of lymphatic vessels and lymph nodes. Ann Vasc Dis 5:145–150.

Rehani, M, Yang, M, Melick, M, et al. (2020). Patients undergoing recurrent CT scans: assessing the magnitude. Eur Radiol 30:1828–1836.

Roach PJ, Schembri GP, Ho Shon IA, Bailey EA, Bailey DL (2006). SPECT/CT imaging using a spiral CT scanner for anatomical localization: impact on

diagnostic accuracy and reporter confidence in clinical practice. Nucl Med Commun 27:977–987.

Rutgers EJ, Donker M, Straver ME et al.(2013). Radiotherapy or surgery of the axilla after a positive sentinel node in breast cancer patients: final analysis of the EORTC AMAROS trial (10981/22023). Presented at the 49th Annual Meeting of the American Society of Clinical Oncology. May 31-June 4, 2013; Chicago, IL. Abstract LBA1001.

Sawyer LJ, Starritt HC, Hiscock SC, Evans MJ (2008). Effective doses to patients from CT acquisitions on the GE Infinia Hawkeye: a comparison of calculation methods. Nucl Med Comm 29:144–149.

Silverman S.G., M.R.M. Sun, K. Tuncali, et al (2004). Three-Dimensional Assessment of MRI-guided Percutaneous Cryotherapy of Liver Metastases‖, Am. J. Roentgenol. 183, 707-712.

Slavin SA, Greene AK, Borud LJ. Lymphedema. In: Weinzweig J, ed. Plastic surgery secrets plus. 2nd ed. Philadelphia, PA: Mosby; 2009.

Stafford R.J., (2005). High Field MRI — Technology, Applications, Safety, and Limitations‖, Med. Phys., vol. 32, 2077.

Sulieman, A, Tammam, N, Alzimami, K, Elnour, A, Babikir, E, Alfuraih, A.(2015). Dose reduction in chest CT examination. Radiat Protec Dosim. 165; (1-4):185–189.

Tsalafoutas, I and Koukourakis,G.(2010). Patient dose considerations in computed tomography examinations. World J Radiol 28(7): 262–268.

Vedrine, G. Aubert, F. Beadet et al. (2010). Iseult/INUMAC Whole-body 11.7 T MRI Magnet Status, IEEE Trans. Appl. Supercond., Vol. 20, 696-701.

Western and Eastern European Market for MRI Frost & Sullivan, Report M3C60-50, 2009.

World Health Organization (2014). Featured map: world: distribution of lymphatic filariasis and status of preventive chemotherapy in endemic countries, 2014.

Wu et al. (2011). Diagnostic performance of USPIO-enhanced MRI for lymph-node metastases in different body regions: A meta-analysis. European Journal of Radiology. 80, (2), 582–589.

Xiao Yu-Dong, Ramchandra Paudel , Jun Liu, Cong Ma , Zi-ShuZhang . Shun-Ke Zhou.(2016). MRI contrast mediums: Classification and application (Review). International Journal of Molecular Medicine. 1319-1326.

Xiong L. et al (2014). Current techniques for lymphatic imaging: State of the art and future perspectives. EJSO 40 (2014) 270-276.

Young KE; Sup PJ, Ho LK; Young HS.(2016). Incidence and Risk Factors of Lower Extremity Lymphedema After Gynecologic Surgery in Ovarian Cancer. International Journal of Gynecological Cancer: 26 (7), 1327–1332.